REMOTE SENSING

Multispectral Analyses of Cultural Resources

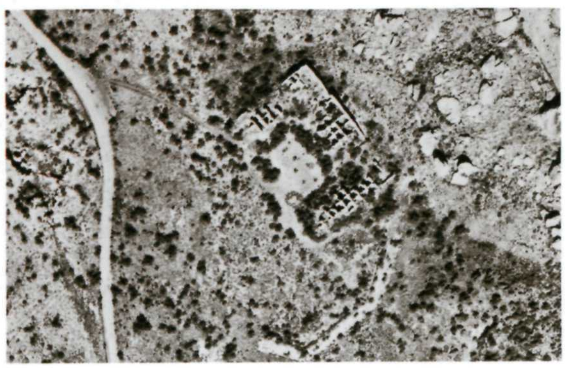

Supplement No. 5

REMOTE SENSING

Multispectral Analyses of Cultural Resources: Chaco Canyon and Bandelier National Monument

Supplement No. 5

to *Remote Sensing: A Handbook for Archeologists and Cultural Resource Managers*

Thomas R. Lyons, Editor

Cultural Resources Management
National Park Service
U.S. Department of the Interior
Washington, D.C.
1981

Library of Congress Cataloging in Publication Data

Main entry under title:

Remote sensing supplement.

Supplements to Remote sensing: a handbook for archelogists and cultural resource managers by T. R. Lyons and T. E. Avery.

1. Aerial photography in archaeology—Collected works. 2. Photography in archaeology—Collected works. I. Lyons, Thomas R. Remote sensing.
CC76.4.LK96 Suppl5 930.1'028 80-81

Cooperating Organizations

National Park Service: Cultural Resources Management Division, Washington Office; Remote Sensing Division, Southwest Cultural Resources Center; University of New Mexico: Technology Application Center

For sale by the
Superintendent of Documents
U.S. Government Printing Office
Washington, D.C. 20402

Preface

This supplement is designed for use with Remote Sensing: A Handbook for Archeologists and Cultural Resource Managers, by Thomas R. Lyons and Thomas Eugene Avery. The handbook may be obtained by writing the Superintendent of Documents, U.S. Government Printing Office, Washington, D.C. 20402.

Within the next several months, the Natioinal Park Service will publish other supplements to the handbook dealing with regional applications of remote sensing for the archeologist and cultural resource manager. The reader may receive notification of these publications as they become available by writing the Superintendent of Documents (address above) and asking to be placed on mailing list N–557.

Contents

PART 1

An Airborne Spectral Analysis of Settlement Sites in Chaco Canyon

Stanley A. Morain
Thomas K. Budge
Amelia Komarek

Contents

Illustrations

Tables

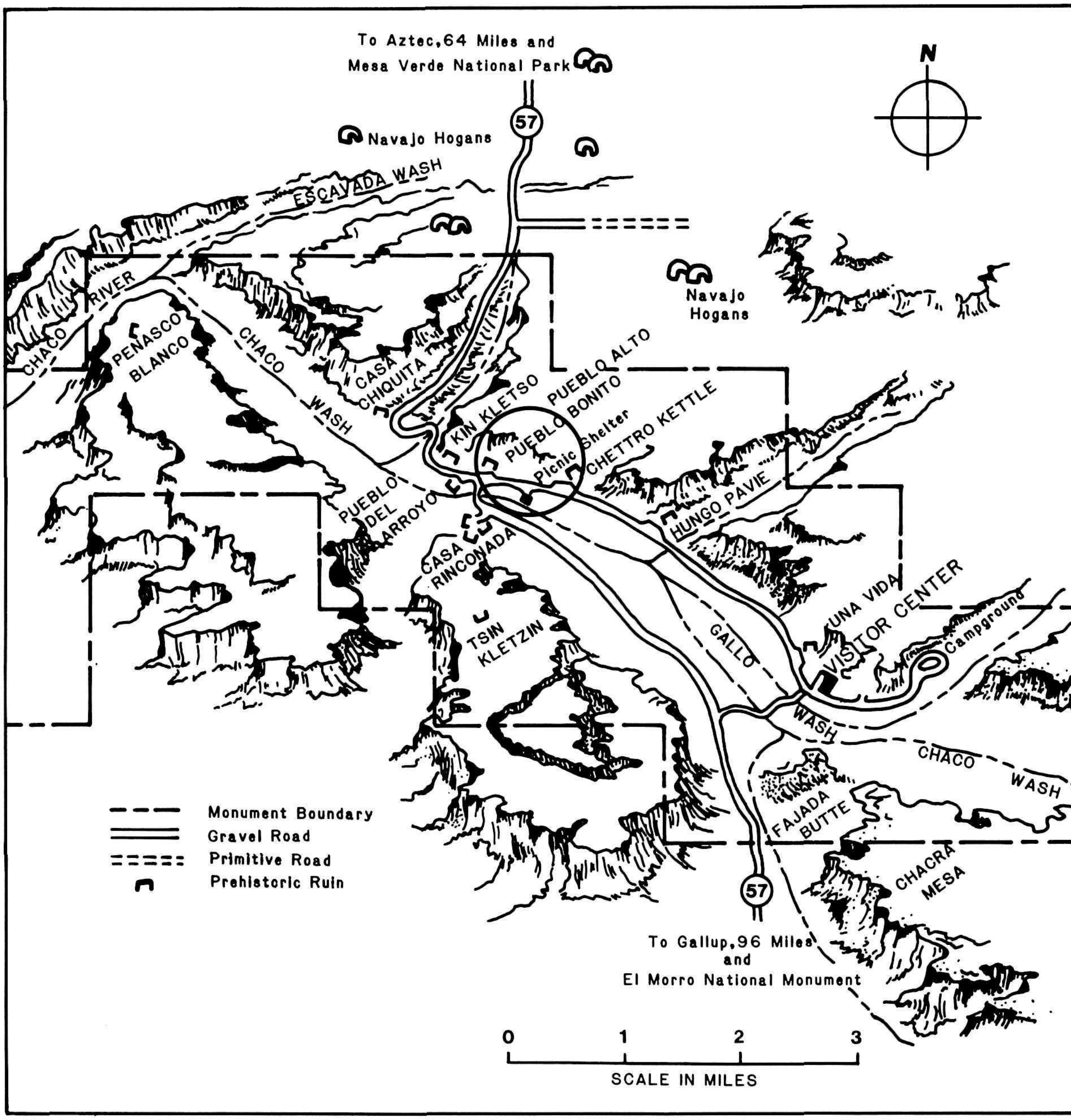

Figure 1 Location map of the prime sites (circled) involved in this study. Kin Bineola and Wijiji are located off the map to the left and right respectively.

Section 1

Introduction

This report describes studies performed in connection with the collection and analysis of multispectral data obtained over Chaco Canyon, New Mexico. Five Anasazi pueblos were the focus of attention in these studies: Pueblo Alto, Kin Bineola, Pueblo Bontio, Chetro Ketl, and Wijiji (fig. 1). During the airborne data collection phase, we provided field support by collecting soil moisture and vegetation structure data at Pueblo Alto, Kin Bineola and Wijiji. Part II of the report describes the procedures used and interpretation of these data.

Upon receipt of the digital data tapes from Bendix, the authors arranged for a two-day computer analysis session at the EROS Data Center in Sioux Falls, South Dakota. Part III of the report describes and illustrates the principal results of this session including some preliminary interpretations and recommendations.

In Part IV, we have attempted to extend the discussions initiated in Parts II and III, in a general sense, and to discuss more fully the specific topics of agricultural fields, prehistoric roads and evidence for archeological structures.

Section 2

Field and Laboratory Studies

Pre-Field Preparations

Selected transects were drawn on lithographic prints of the study areas.* The longest transect was 275m and the shortest transect was 35m. Transects were chosen on the basis of tonal changes relating to vegetation density, soils, roads, and other landscape features. Sampling sites were then chosen along each transect to coincide with apparent soil and vegetation changes. At the Kin Bineola study area, special effort was made to include areas of heat anomalies shown on thermal scan imagery supplied by the Chaco Center.

Soil Sample Collection

Before actual sampling began, the study sites were checked to insure that the transects drawn and the sites selected along those transects adequately represented areas of change. Using a small hand shovel and plastic bags with tape for labeling, soil samples were taken along the transects. As the samples were taken, the bags were labeled to correspond to the soil sample site plotted on the lithograph. The labels indicated the transect, location number and whether it was a surface or subsurface sample. One hundred twenty (120) samples were taken at Pueblo Alto, sixty four (64) at Kin Bineola, and thirty (30) at Wijiji.

A surface and subsurface sample were taken at each location. Each surface sample was taken by collecting the top 1.25 cm to 2.5cm of soil in at least four places within arm's reach.

The subsurface sample was taken at about 15cm and placed into a plastic bag that was labeled and tied like the surface samples. For the most part, subsurface samples were drier.

Soil Moisture Determinations and Interpretation

A table was prepared to record data as shown in Table 1. It included space for identifying the study site, locating the sample, identifying the can number, sample number, wet soil weight, dry soil weight, weight difference and percentage of moisture contained in the sample.

Soil cans with lids were obtained and labeled to correspond to sample identifications. The tare weight for each was then obtained using a Mettler balance. Twenty-five grams of "wet" soil were added to the cans and placed in an Acme Laboratory drying oven at 105° C for 24 hours. This temperature is high enough to drive off any capillary water (water between and around sand grains), but low enough to retain any water chemically bonded to the sand components. After 24 hours, all cans were removed from the oven, weighed and recorded. This weight was referred to as the dry weight. By subtracting the dry weight from the original "wet" weight, the water lost on drying was determined. To figure the percentage of moisture in each sample, the following equation was used:

$$\%\ \text{moisture} = \frac{\text{weight lost on drying}}{\text{weight of dry soil}} \times 100$$

*Pueblo Alto study area was 182,400m^2
Kin Bineola study area was 361,254m^2

Table 1: Data form for calculating soil moisture.

Top sample______ Bottom sample______

Location______________________. Date______________.

Can No.	Soil Sample No.	Soil Weight (wet)	Soil Weight (dry)	Weight Difference	% Moist

Soil moisture percentages for each surface and subsurface sample are given in Appendix A.

Figure 2A,B shows Bendix Channel 11 (thermal scan) imagery for the Pueblo Alto and Kin Bineola sites, upon which are plotted the location of the soil sample transects. Table 2 lists the average sample-to-sample moisture variation along each transect as well as the grand (overall) average between all samples at each site. It is apparent that, on the day of the overflight, soil moisture differences at the surface were too small to relate to meaningful differences in soil temperature. Figure 2A (Pueblo Alto) shows almost no gray scale variation across the scene. This is not surprising since the average moisture variation is less than 1 percent. At Kin Bineola (fig. 2B), the overall average variation is 1.29 percent and there are some vague tonal patterns evident. A closer look, however, reveals that vegetation is the key parameter affecting surface temperature.

Phytocenological Records

Using 6—meter—square quadrants, a series of phytocenological records was prepared along the soil transects. Table 3 is the form utilized for that effort and was extracted from Küchler (1967, p.195). These data in the final analysis were of no assistance. Vegetation patterns, however, are clearly visible on Channels 2 through 10 of the Bendix Data and are espeically valuable in aiding the delineation of agricultural fields and prehistoric roads. The reason the phytocenological records are of no use is because the field teams had to select the sites *a priori* and secondly (perhaps most importantly), for archeological investigations, species composition may be more important than density. See Figures 7 and 16 for more discussion on this topic.

Table 2. Moisture Variations Along Transects at Pueblo Alto and Kin Bineola (See Figure 2 for transect locations).

	Transect	Average Sample-to-Sample Moisture Difference (%)
	Pueblo Alto	(Grand average .83%)
	A	1.54
	B	.44
	C	.57
	D	.89
	E	.07
	F	.57
	G	.63
	H	1.55
	J	1.19
	Kin Bineola	(Grand average 1.29%)
	A	1.24
	B	.54
	C	1.34
	D	.84
	E	1.17
	F	.75
not shown on figure	G	1.58
	H	2.85

A

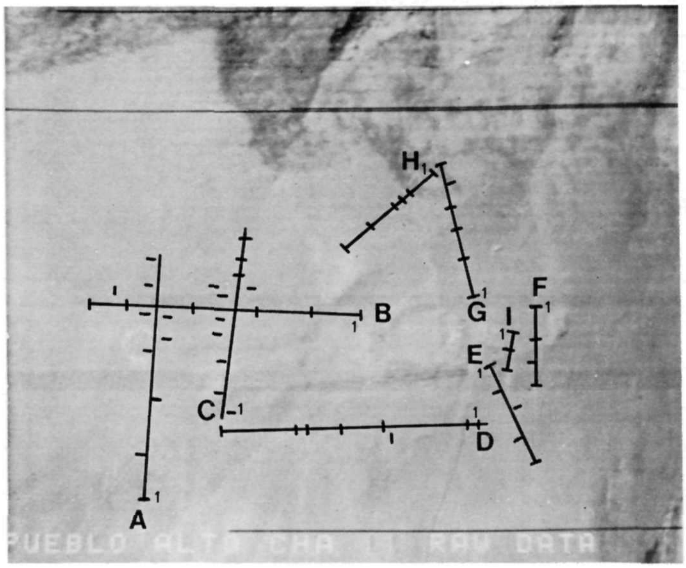

B

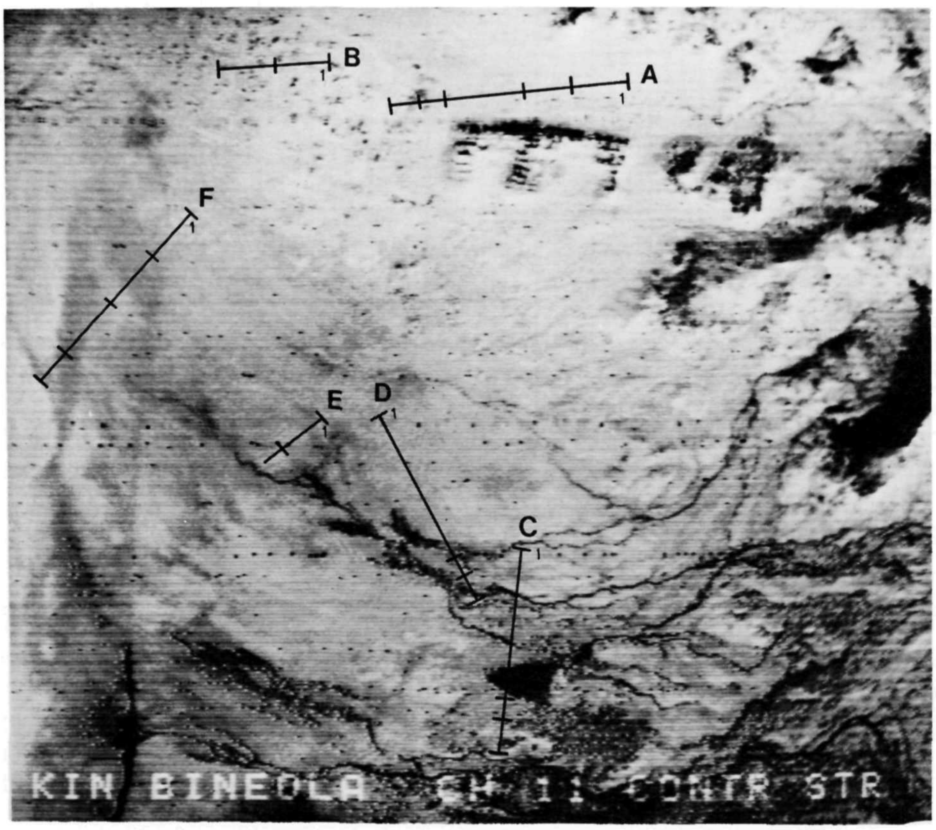

Figure 2 Thermal scan images (Bendix Channel 11) of Pueblo Alto (A) and Kin Bineola (B) sites. Transect lines have been superimposed to show locations of soil moisture and vegetation structure sampling sites.

Table 3. Data Form for Phytocenological Record

PHYTOCENOLOGICAL RECORD No. ____

Location: ____

Height above sea level: ____

Slope and exposure: ____

Landscape: ____

____

Date: ____

Base Map; ____

Aerial photograph No. ____

Type (transect, quadrat, etc.) and size of stand samples: ____

Structural Analysis

Height classes: / Life forms:	B broadleaf evergreen	D broadleaf deciduous	E needleleaf evergreen	N needleleaf deciduous	O aphyllous	S B + D semi-deciduous	M D + E mixed	G graminoids	H forbs	L lichens mosses	C climbers (lianas)	K stem succulents	P palms	T tuft plants	V bamboos	X epiphytes
8 = > 35 meters																
7 = 20 - 35 "																
6 = 10 - 20 "																
5 = 5 - 10 "																
4 = 2 - 5 "																
3 = 0.5 - 2 "																
2 = 0.1 - 0.5 "																
1 = < 0.1 "																

coverage: c = > 75%; i = 51 – 75%; p = 26 – 50%; r = 6 – 25%; b = 1 – 5%; a = < 1%.

leaves: h = hard (sclerophyll); w = soft; k = succulent; l = large (> 400cm²); s = small (< 4cm²).

Notes

Section 3

Data and Image Processing

The Bendix M^2S Scanner

On October 19, 1976, a Bendix M^2S multispectral scanner (fig. 3) was flown over Chaco Canyon at an altitude above terrain of 1500 feet (approx. 500 meters). Eleven channels of data were collected, as listed in Table 4. Of these, Channels 2 through 11 provided usable data for processing.

All data were collected in digital form with a spatial resolution (IFOV) of 3.75 feet. The channels have slightly different performances in terms of their spectral response, but in all but one case, noise equivalent changes in reflectances (NE$\Delta\rho$) are less than 1 percent. This is considered to be excellent in subhumid and humid environments where variations of 50 percent or more are observed in natural scenes. Based on the relatively low image contrasts observed in the Chaco data, however, one wonders whether these sensitivities are sufficient to record extremely subtle reflectances in sparsely vegetated arid zones.

Average M^2S channel performances are given in Table 5. The values are averages of six separate scanners tested in the Bendix laboratory. The higher the values, the less sensitive the channel to spectral changes in the landscape. Channel 11 (the thermal infrared band) is sensitive to landscape temperature differences (NEΔT) of about 0.1° C.

Figure 4 illustrates the visual appearance of data from Channels 2 through 11, as displayed directly from the tapes without alteration. Each image was photographed from the GE Image-100 output screen which has a standard resolution of 512 lines. To optimize the resolution of the M^2S and Image-100 systems, therefore, only 512 lines and 512 pixels* of scanner data were displayed for each channel.

The GE Image-100 Multispectral Image Processor

For data analysis, we utilized the Department of Interior EROS Data Center facilities in Sioux Falls, South Dakota. The Data Analysis Lab is equipped with a General Electric Image-100 processor, an ESL IDEMS system and a digicolor film recording system, together with appropriate software. For the Chaco Canyon studies, we utilized the Image-100 techniques solely, with the exception of one image (the cover photo) processed by film recording as a demonstration of capability.

The Image-100 is described as an interactive digital image analysis package. It is "interactive" in the sense that it consists of specified analytical techniques which can be performed in any sequence at the request of the analyst. The video display output is controlled by the analyst by simply answering questions displayed on the control consol by the computer. The basic system is shown in Figure 5.

For the Chaco Canyon project, we mounted the digital data tapes for flight lines containing areas of interest (primarily Pueblo Alto, Kin Bineola, Wijiji, Chetro Ketl and Pueblo Bonito). Using strip images provided by Bendix for each of the flight lines, we estimated the scan line and sam-

* "Pixels" are picture elements or individual resolution cells along a scan line. They are also referred to as samples.

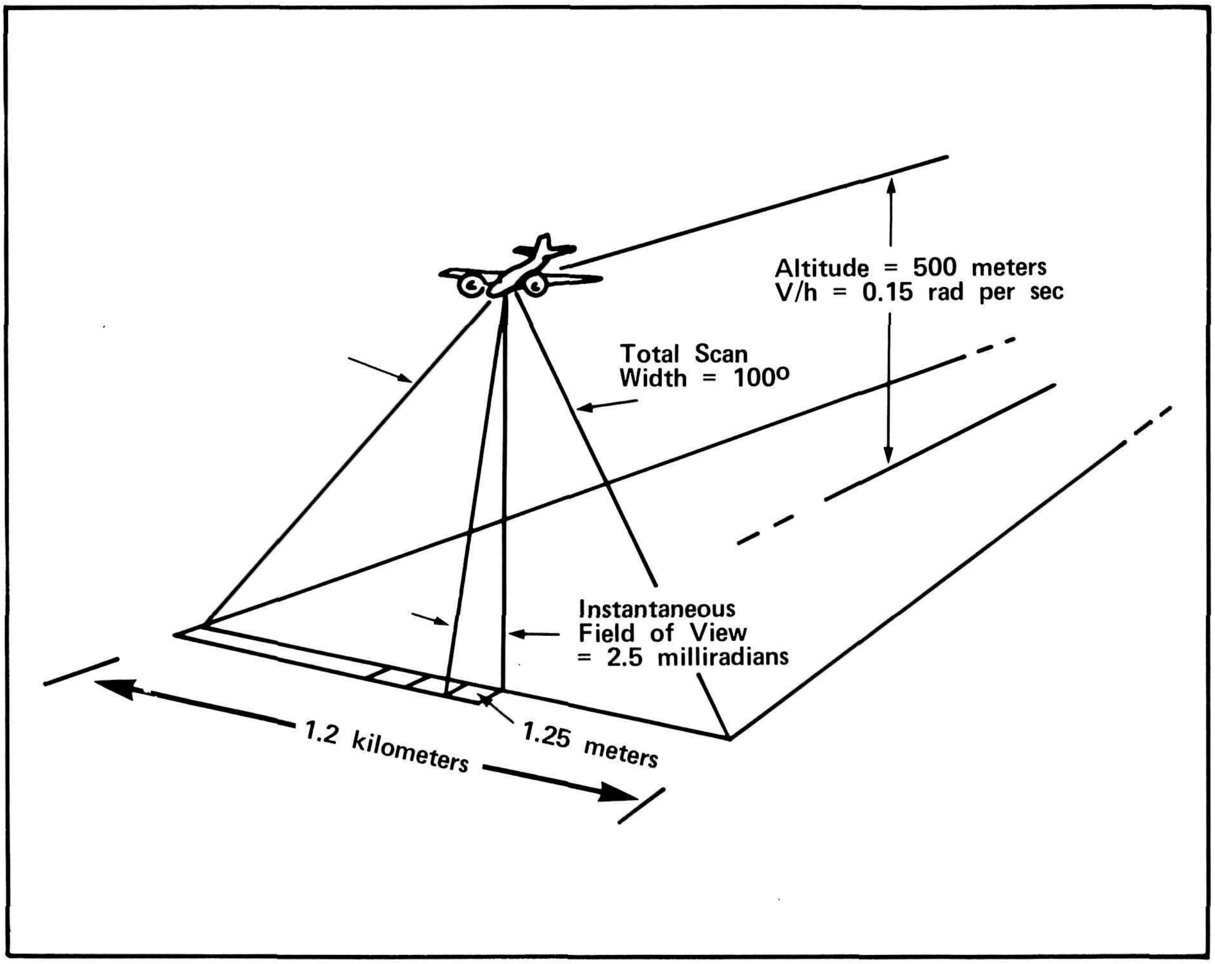

Figure 3 Schematic of the Bendix M^2S system as it was actually flown over Chaco Canyon. Reflected radiation was recorded over a 100° field of view with an instantaneous field of view of 2.5 milliradians. These are equivalent to a ground swath width of 1.2 kilometers (3000 feet) and a resolution cell of 1.25 meters (3.75 feet). With an aircraft speed of 75 meters/sec the velocity-to-height (V/h) ratio was 0.15 radians/sec. Radiation from the ground falls incident upon a rotating mirror in the aircraft and is partitioned into eleven channels. For complete details of the M^2S design and operation see Bendix B5R 4167A dated December 1975.

ple number of the upper left corner of an area to be displayed, and entering these numbers in control consol, displayed in sequence the eleven channels of spectral data for that area (see fig. 4). Since the image analyzer can only store and manipulate four channels at a time, however, it was necessary to subjectively select the "best" four out of the eleven for analysis at any time. In practice, only three channels can be effectively analyzed at once in order to leave the fourth channel open for displaying enhancements and ratios of the other three.

Analysis Techniques

The aim of image enhancements is to provide a simpler, clearer or more interpretable image. Certain functions can be considered as essentially "cosmetic," while others actually recombine digital data into a "new" picture that must then be interpreted for its information content. Lastly, there are some display options that assist in supplying "ready-made" illustrations for slide or hard copy products.

Table 4. Spectral channels, bandwidths and equivalent spectral colors of the Bendix M^2S scanner.

Channel	Wavelength (nanometers) Center λc	Bandwidth $\Delta\lambda$	Equivalent Spectral Color
1	410	060	violet
2	465	050	blue
3	515	050	green
4	560	040	yellow green
5	600	040	orange
6	640	040	red orange
7	680	040	red
8	720	040	reflective IR
9	815	090	reflective IR
10	1015	090	reflective IR
11	1100	2.5	thermal IR

Table 5. Average M^2S Performance

Channel	$NE\Delta\rho$
1	1.26%
2	.26
3	.18
4	.21
5	.21
6	.19
7	.20
8	.25
9	.23
10	.52
11	($NE\Delta T$) .12° C

The total combination of options intersected with the vast amount of digital data collected over Chaco, and in turn intersected with the 3-channel, 512—scan line option we chose for display, means that only a fraction of the potential analysis techniques and options have been performed.

"Cosmetic" Processing

There are two functions that can be performed to visually improve the appearance of raw images. One is a clean-up operation that replaces missing scan line data by averaging the scan lines above and below it. The other is referred to as contrast stretching.

Data "clean-up". The clean-up operation is performed on the video display consol by moving a cursor to the line of missing data. By commands given through the control consol, the spectral data for the bounding scan lines are inspected and averaged sample-by-sample. A new line of data is created for the missing line and stored along with the rest of the image in the memory module. The original data tape is not altered in any way by the process.

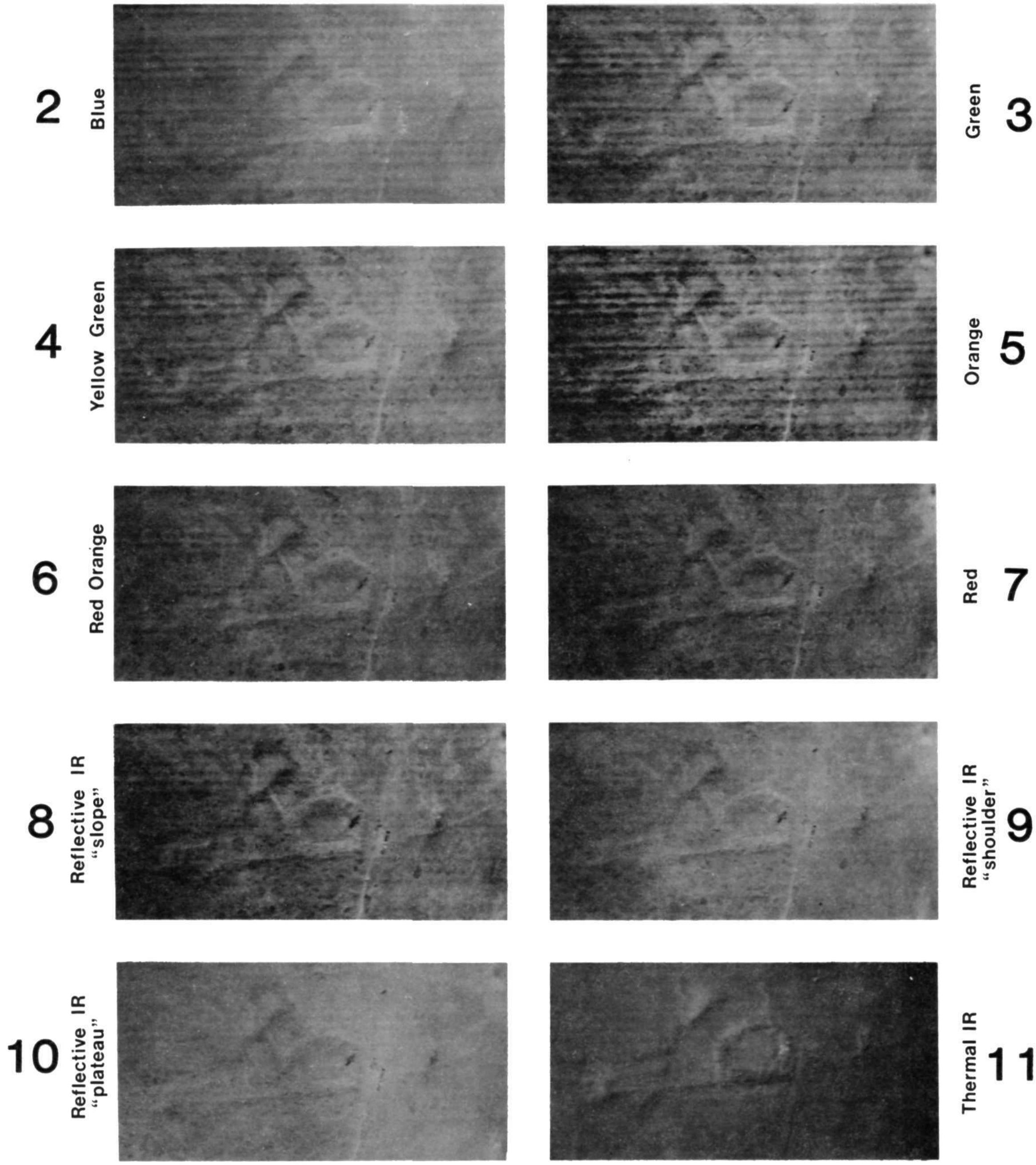

Figure 4 Typical M^2S digital-to-image output for an area around Pueblo Alto. Slight differences in gray scale are due to gain and brightness adjustments during video display. Due to photo trimming, each image as shown here contains approximately 235 scan lines and 425 samples; an area on the ground equivalent to 880 feet by 1595 feet (1″ = 587 feet). The words "slope", "shoulder", and "plateau" refer to the typical reflected IR curve for vigorous vegetation.

Figure 5 The Image-100 image analyzer consists of a control console and graphics display terminal (A) where commands are taken and returned by the system or where histograms can be displayed; magnetic tape drives (off the picture to the right); a PDP 11/35 computer (B); a solid-state memory module (C); an input scanner (D) and a video display unit (E) containing the image enhancement control panel. The analyst alternates his activity between the control console and image enhancement panel, as seen here. Analysts can learn to use the system effectively in a few hours.

Figure 6 illustrates a before-and-after scene of Pueblo Alto. The black lines on 6A represent missing data. They have been removed on 6B by the process described. The Bendix data analyzed for this study were remarkably free of such problems; and, in fact, only Channels 10 and 11 required much, if any, clean-up.

The clean-up operation introduces false data into the scene. If the number of missing lines is not large and they are widely spaced, then little practical damage is suffered for most applications at this resolution. The damage could be serious in archeological studies if the intent were to locate narrow linear features like walls, ditches or trails oriented parallel to the scan path (perpendicular to the line of flight).

Contrast stretching. Reference to Figure 4 indicates that some of the original data appears to be "washed-out" or to have a narrow range of gray tone values. Using a variety of mathematical functions, the contrast can be widened or "stretched" before other enhancement activities are performed. The process of contrast stretching involves changing, by a prescribed amount, the digital values for all, or a selected set of samples in a given channel or image data. It is not the same as simply altering the brightness or contrast settings on the enhancement control panel.

The basis for all contrast stretch functions is the image histogram. Using a rectangular cursor located over an area of the image having critical importance, the computer scans the enclosed data

A

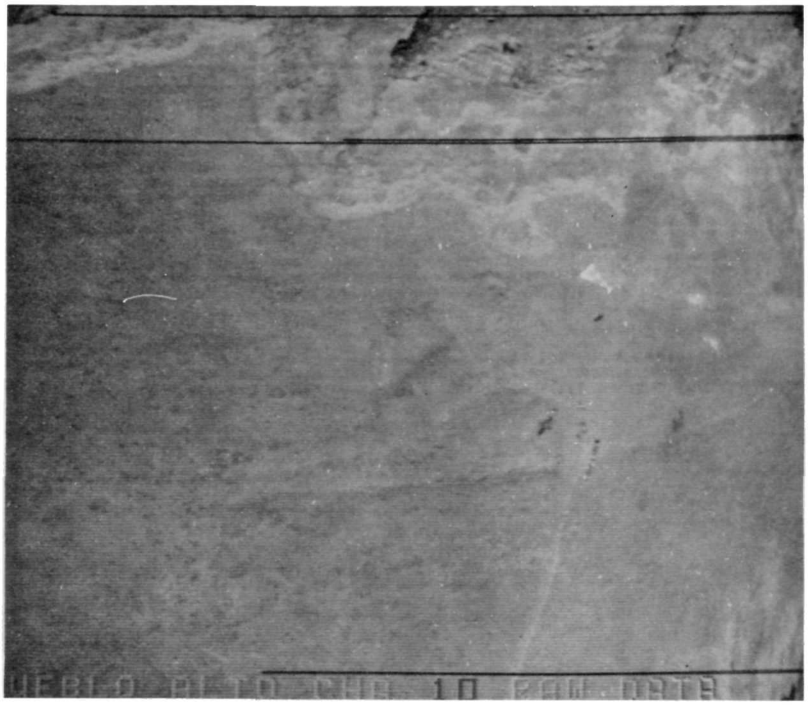

B

Figure 6 Data "clean-up" can be accomplished by replacing missing scan lines (black lines in A) with artificial scan lines created by averaging the values above and below. This operation is done on the video display unit and stored in the memory module to avoid altering the original data tape.

and creates a graph of frequency Vs gray level. The result is then displayed on the control consol and can be printed in hard copy for future reference. Figure 7 shows raw and stretched images for the red-orange and thermal infrared channels over Pueblo Alto, together with their before-and-after histograms.

For the red-orange data (fig. 7A,B) the original range of gray tones was 167 out of a possible 256. The range spread from gray level 89 (light gray) to 255 (black). In the stretched version, the histogram has been spread from gray level 2 to 254 and the mean has been shifted from level 158 to level 107. In terms of image appearance, there has been a shift toward more light tones and more dark gray tones. In the process of stretching the tones around Pueblo Alto, the tones at left of the photo in 7D have become saturated black and those along the scarps at the top have become saturated white.

A similar result is observed for the thermal infrared sequence (fig. 7E-H). Enhancement of the Pueblo Alto site has obscured data for the surrounding region.

All of the contrast stretching performed for the Chaco Canyon sites is described as simple linear stretching. Pixel values are reassigned by a constant value either up or down to spread the range. Other options include nonlinear stretches using a logarithmic or Gaussian function. These take more computer time to calculate and more analyst interaction to determine upper and lower gray scale limits. We did not believe the extra time was warranted in view of the exploratory nature of our analysis and time constraints on the machine.

Image Enhancement Techniques

Once the scan line data have been cleaned up and the images contrast stretched,* they can be enhanced and displayed using a variety of strategies. Among the more common options are:

a) color combinations of 2 or more channels;
b) theme extraction;
c) band ratioing; and
d) spatial filtering.

All of these activities were performed for sites in Chaco Canyon on an extremely limited basis and we recommend that the studies be expanded to include more areas in the data set.

Color combinations. The image enhancement control panel is the prime unit for this activity. By depressing combinations of channel and color selector buttons, virtually any display of spectral data can be shown in what is termed a "false color composite" (fcc).

Figure 8A shows a three channel composite of blue spectral data (Channel 2) displayed by the red color gun of the TV, reflective infrared (Channel 8) by the green gun, and thermal infrared (Channel 11) by the blue gun. The clarity of the resulting image attests to the extremely close registration of sample values between the three channels.

The purpose of such combinations is to facilitate interpretation of several images at once and to highlight, or enhance, features that might otherwise not be evident. Selection of the spectral channels for such a comparison is based on knowledge of the general reflectances of landscape elements.

In Figure 8A, for example, the combination of blue data with thermal data should enhance soil moisture features because reflectance values decline in both channels as moisture increases*. Relatively more moist areas should appear darker than relatively drier areas. This basic interpretation is confirmed by comparing the darker blue tones of Chaco River valley with those of the drier mesa top.

With specific regard to the Chetro Ketl site, the following observations are made:

i) The blue-green areas at A suggest the presence of unearthed kivas. These are not evident in Figure 8B.
ii) Item B is a confirmed prehistoric road leading from Chetro Ketl to Pueblo Alto. Whether or not this color and spectral combination would be equally indicative of roads elsewhere in the canyon should be investigated.
iii) The general area marked C may contain some buried walls or other structures. There is a vague hint of other kivas contained within a more or less rectangular area. Reference to the same area on 8B also suggests the presence of structures.
iv) The area of light blue along the scarp represents colluvial deposits. They are

* It is not always necessary to perform the stretch function.

* The high specific heat of water compared to soil mineral material causes moist soil to heat up and cool off more slowly than dry soil. The statement made above is only true during daytime sensing. At night, a moist soil, being warmer, would appear relatively brighter than surrounding drier soils.

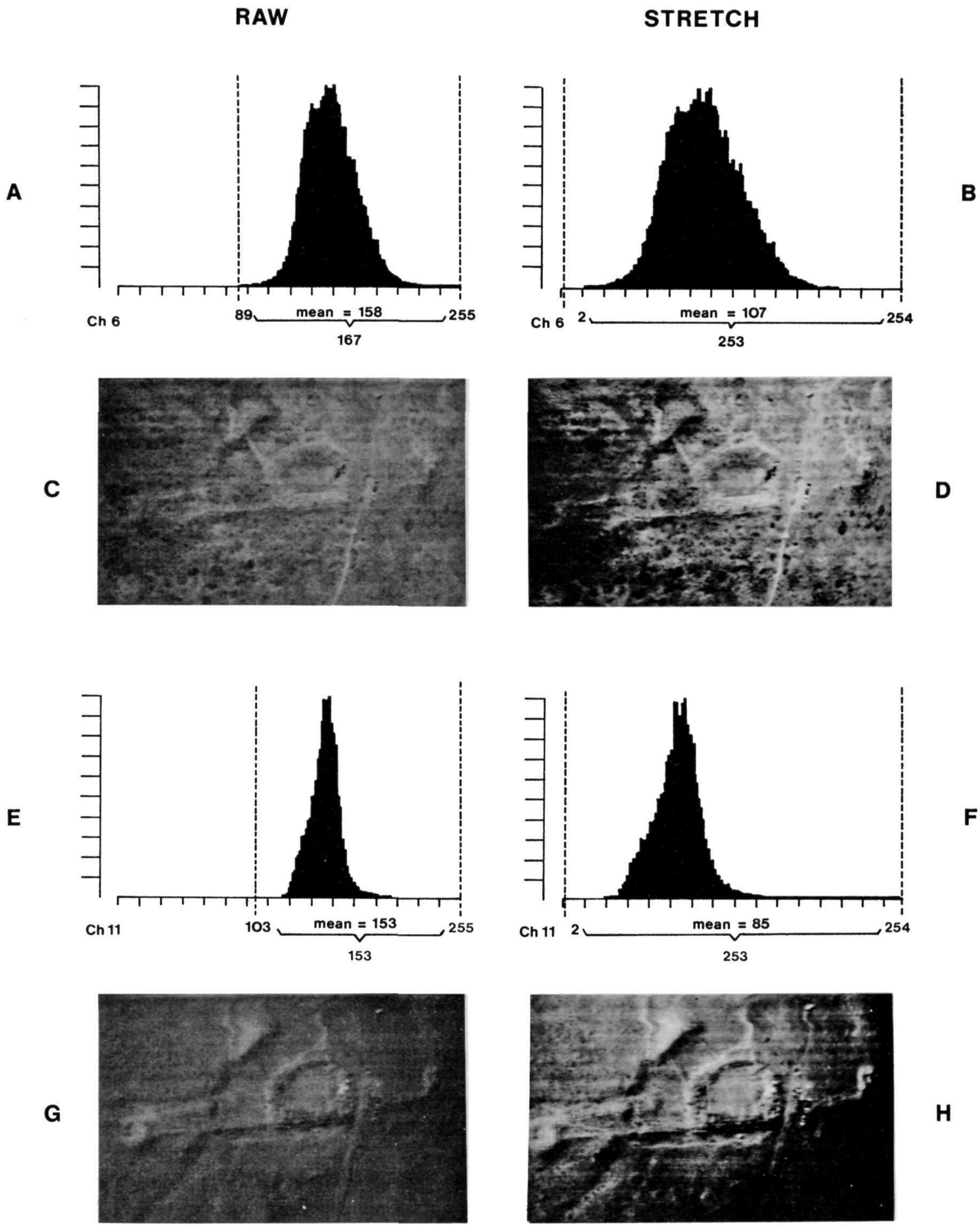

Figure 7 The process of linear contrast stretching involves the alteration of the gray tone histogram and a corresponding reassignment of values to image pixels. See text for more detailed discussion.

distinct because of slope orientation, not because of any unique composition or moisture content.

Figure 9 is a different approach to color combination. It represents the only instance where we compressed the digital image data by showing more than 512 scan lines. The area shown includes Chetro Ketl and Pueblo Bonito, and much of the scarpland leading to Pueblo Alto. It is a tri-color composite but utilizes only two channels of data—2 (blue) and 11 (thermal infrared)—combined as given below:

Channel	*Displayed In*
2	red
11	blue
11	green

A few items have been highlighted for consideration; however, the overall informational content seems to be low. Confirmed prehistoric roads cannot be detected; nor, at first review, are there any patterns worthy of note.

i) The area marked A stands out because of subtle differences in vegetation speciation and/or density. Its shape and location between the two settlement sites may indicate a previous concentration of agricultural activity.
ii) The area at B has a faint circularity containing an inner and outer ring.
iii) At C, there is a distinctive horseshoe which could be an old meander. It may also be that the interior of the horseshoe is more critical as a possible old field than the horseshoe itself.

Theme extraction. The object of theme extraction strategies is to classify an image into its useful categories for a given application. For some applications, particularly in hydrology, a single theme may be all that is desired (for example the mapping of surface water); whereas in others, like land-use mapping, the entire scene needs to be classified. For our studies at Chaco Canyon, most of the features of interest were only a few resolution elements in size or were linear. There seem to be no point in classifying entire scenes, but there were a few instances where single theme extraction proved interesting.

The process of theme extraction most often involves the placement of a cursor over a known area of a desired category. This is referred to as the "training site," and the computer is then asked to create a set of statistics from the digital values within that area. On the assumption that this training area is typical of the whole category, the remainder of the scene having those same statistics is then "alarmed" and stored for future display in a unique color.

If the size of the training site is not easily known to the analyst; or, if much of the scene appears to have the same gray tone, then a two dimensional projection of the digital values (or stretched digital values) can be displayed as a graphic on the control consol. The size, shape, and location of the cursor can then be manually altered to include only chosen gray tones. By reviewing the TV monitor, the total image area having those gray tones can be seen. Figure 10 is an example of the graphics displayed for this approach.

Figure 10B illustrates the extraction of a single theme (red) from the combination of two channels of data (blue background). The stimulus for selecting this particular theme arose out of an observation of a faint "halo-like" region around Pueblo Alto. The distribution of red *does* suggest a faint halo but is also seen to extend along the entire scarp front behind Pueblo Bontio and Chetro Ketl.

In searching for the meaning of such a halo (if it really exists), we are reminded of similar occurrences reported in the Russian literature on the topic of "Takyr" soil. These are an anthropogenic form of saline (possibly solonchak) soil associated with long—abandoned human settlement. Takyr soils often have a polyonally patterned crust covering the sites of ruined cities in central Asia, (Gourevitch, A., 1963).

The soils at Pueblo Alto are too sandy to have formed a polygonal crust, and, to the authors' knowledge, the chemistry of their salt content has never been studied. However, one could assume that human activity was concentrated in and around the settlement and might even have extended along the scarp front leading to the valley settlements. It is interesting to note in this regard that a faintly lighter shade of blue surrounds the site of Chetro Ketl in Figure 9.

Channel (band) ratioing. The philosophy of ratioing two channels of spectral data resides with a desire to reduce or eliminate redundant information. In Figure 11A, for example, suppose that a terrain element (soil type A) has a reflectance level of 165 in Channel 6 (red-orange) and 180 in Channel 8; soil type B, on the other hand, has a level of 125 in Channel 6 and 140 in Channel 8. Under these circumstances, the slopes on the two

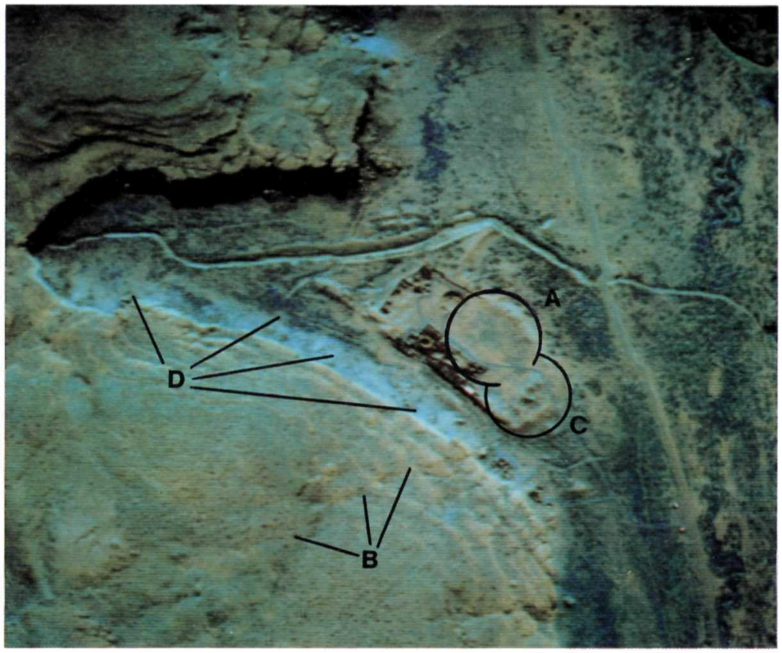

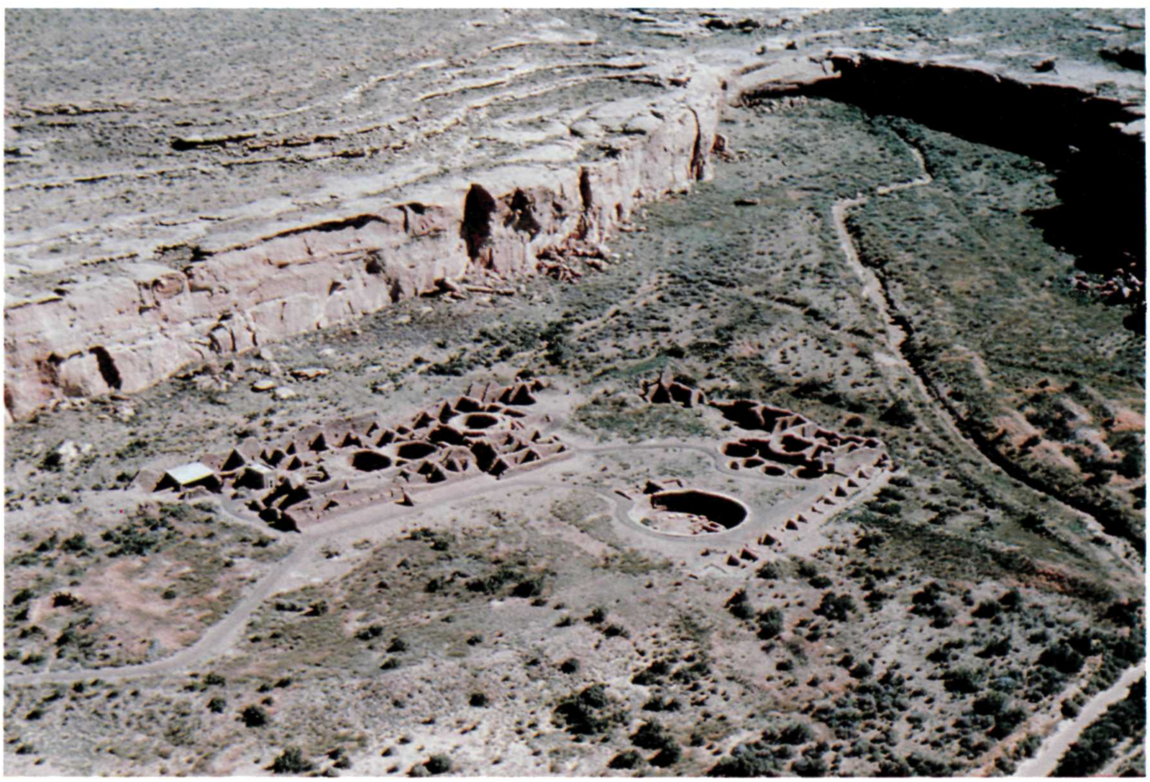

Figure 8 (Above) Blue, reflective infrared and thermal infrared color combination of Chetro Ketl. (Below) Oblique aerial view for use in comparing areas indicated by letters. See text for discussion.

Figure 9 False color composite of Chetro Ketl-Pueblo Bonito area. See text for discussion.

curves are identical and ratioing 6 with 8 would have little advantage.

If, now, equal moisture is added to these soil types and their reflectances drop differentially (fig. 11B), these differences can be enhanced by a ratioing process. This moisture difference can be mapped because the two soil types react differently to the same stimulus.

The above argument is valid for plotting multitemporal differences, but the data for Chaco Canyon is for a single date. For this reason, it becomes almost impossible to interpret any given ratio not generated for a specific purpose. Figure 12 is a ratio generated for Pueblo Alto by dividing the pixel values for the reflective infrared (Channel 10) by the thermal infrared (Channel 11). The result indicates that there is a difference in the strength of reflectance between the structures at A, B and C; and that the trash heap at D is most like the structure at C. What any of this means is not at all clear!

Spatial filtering. Two kinds of data filtering can be accomplished on the Image-100 processor, 1) low pass or smoothing filters, and 2) high pass or edge enhancing filters. Spatial filtering adjusts the value of a pixel with respect to the values of neighboring pixels. A low-pass filter enhances spatial features of a continuous nature which show variation in an area larger than the neighborhood.

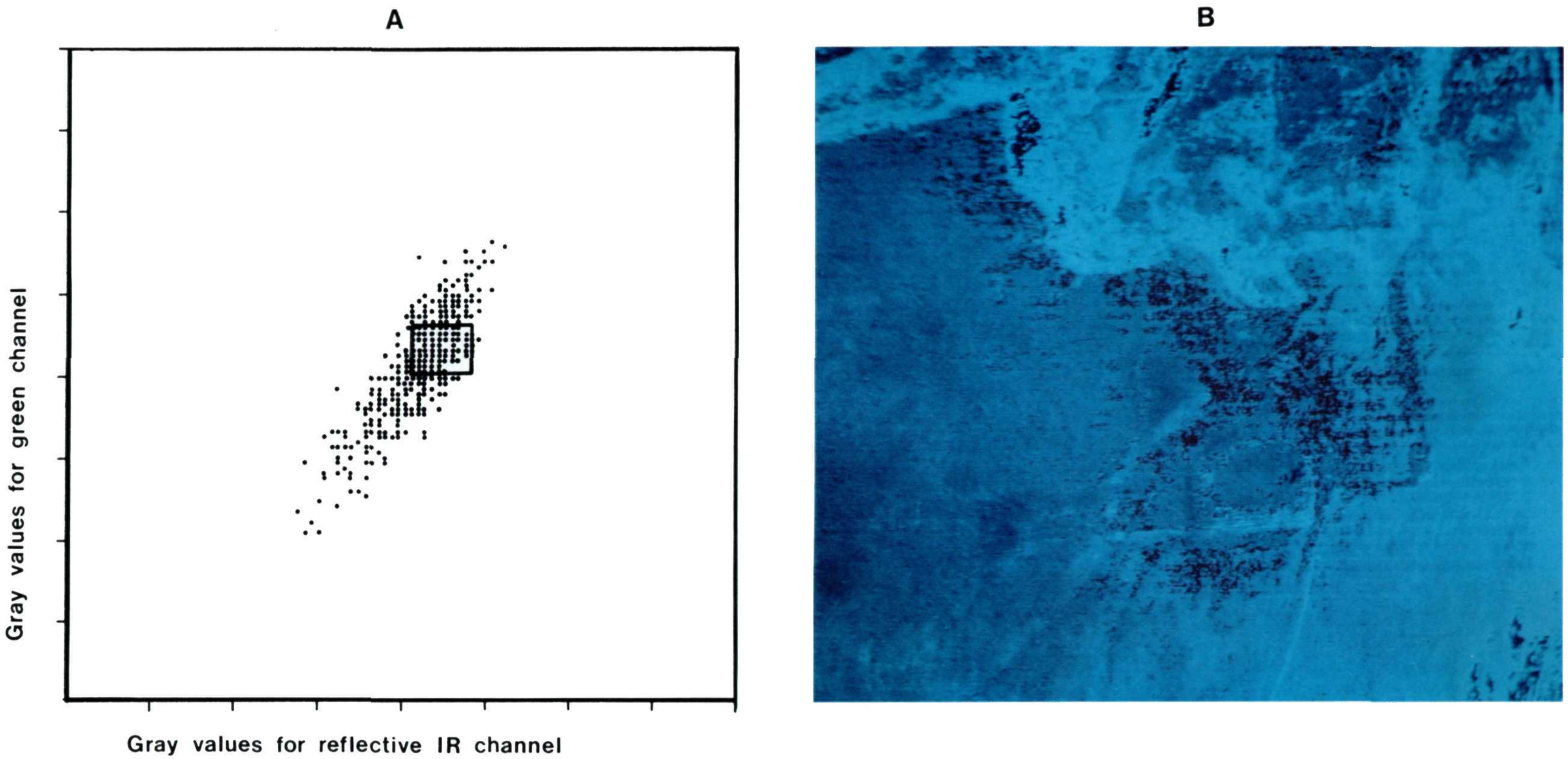

Figure 10 (A) Example of a graphic display of gray tones for channels 3 (green) and 8 (reflective IR). The box shows the location of the cursor. The bounded values are then displayed on the video output in any desired color. The red category in (B) is a single theme extracted by this technique. We found in our studies of the Chaco Canyon area that extremely modest increases in cursor area could equate to vast increases in area catagorized. A great deal of study needs to be undertaken to better understand this problem.

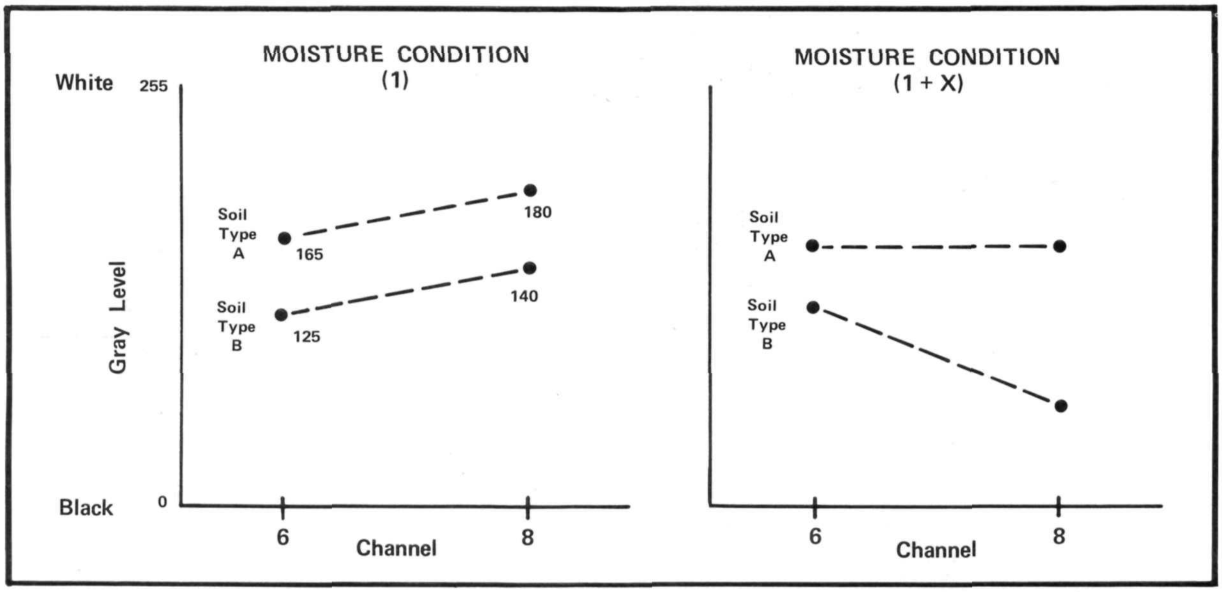

Figure 11 Hypothetical reflectance data for two soil types under two moisture conditions. Under moisture condition 1, the relative difference between soil types for the two channels is identical (the slopes are the same). Under this condition, ratioing the two channels may reveal nothing. Under moisture condition 2, however, the reflectance of soil type 2 declines more than does that for soil type 1. Since the slopes are not the same, a ratio of the two channels should enable differentiation of the two soil types.

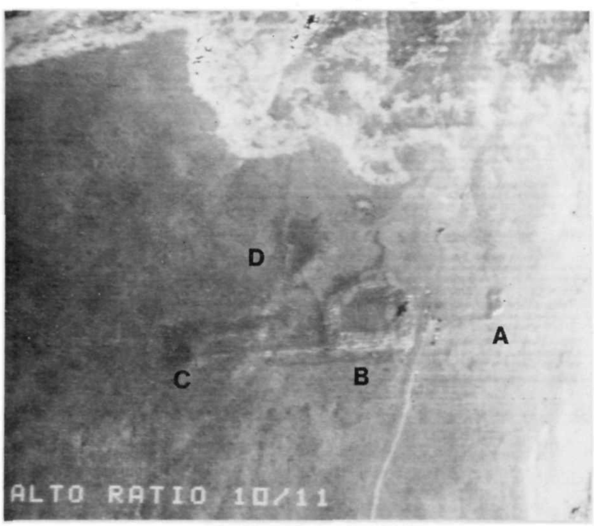

Figure 12 Example of simple band ratio generated by dividing the reflective infrared data from Bendix M²S Channel 10 by the thermal infrared data in Channel 11.

A

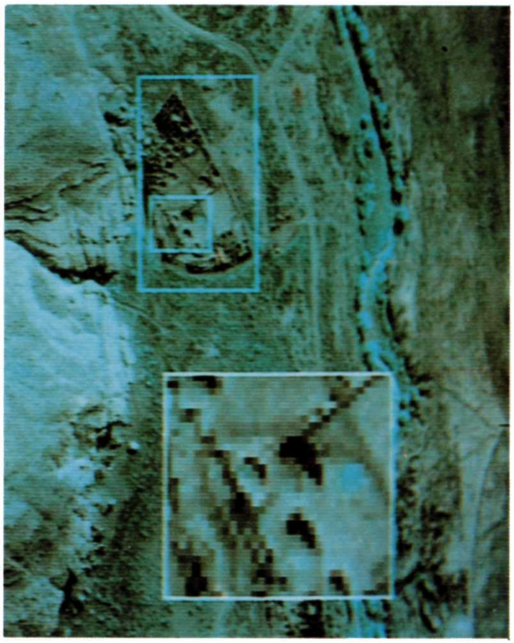

unfiltered

B

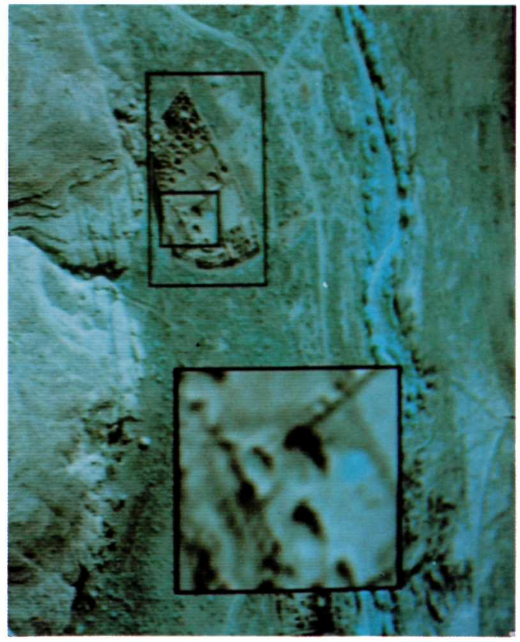

low pass filter

Figure 13 Example of data filtering. The blocky appearance of the enlarged portion of A results from enlarging the pixel size 4-times. Within this area there are several kivas which are lost, for the most part, to visual recognition because of the blockiness. By performing a $\frac{\sin X}{X}$ transformation of pixel values, the blockiness can be "smoothed," as in B, to permit easier pattern recognition. Although the filtered version appears to be somewhat out of focus, it is easier to discern the kiva structures.

High-pass filters enhance features of a discrete nature which show variation in an area smaller than the neighborhood. For our studies of the Chaco Canyon data, only low—pass filtering was explored. Certainly high pass filtering should be studied of *all* the data collected to determine or verify prehistoric roads and to search for agricultural field boundaries.

Figure 13 is an example of the utility of low—pass filtering. In the Anasazi culture, specifically, the technique could be useful in searching out kivas and other circular features like the hogans of later Navajo settlement. Even a casual interpretation of low altitude aerial black and white photographs reveals the presence of circular features equivalent in size to kivas and hogans. A systematic analysis of the valley might pinpoint a number of yet unknown features like this.

Display and Illustration Options.

Since the object of image analysis is to generate interpretable images, most modern processing units have built-in capabilities for annotating and reproducing images off the TV monitor. The Image-100 is particularly flexible in this regard in that annotations, arrows, etc. can be stored on Channel 5 of the output device and called up when a final photograph is desired.

The sequence of photographs in Figure 14 shows a progression of activities leading toward a final illustration. The objective of the exercise was to generate a 2-time enlargement of Pueblo Bonito. This was a unique excercise for the Chaco Canyon analysis since limitations on the machine's capability required the enlargement to be performed in two stages. A perfect fit of the two pieces therefore required juxtaposing exact scan lines and sample numbers.

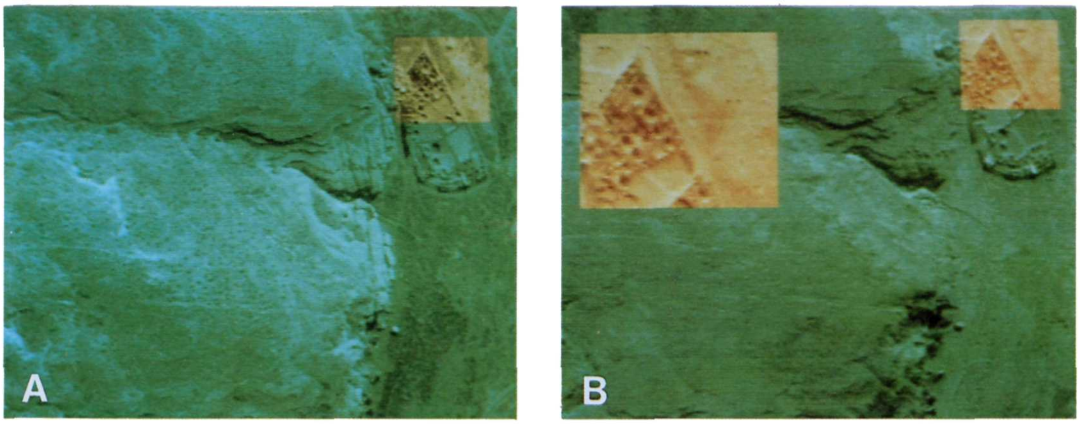

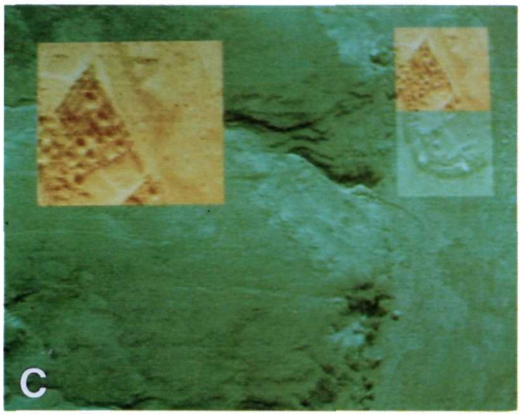

Figure 14 Example of a four step sequence in creating an enlarged and annotated illustration of Pueblo Bonito. See text for explanation.

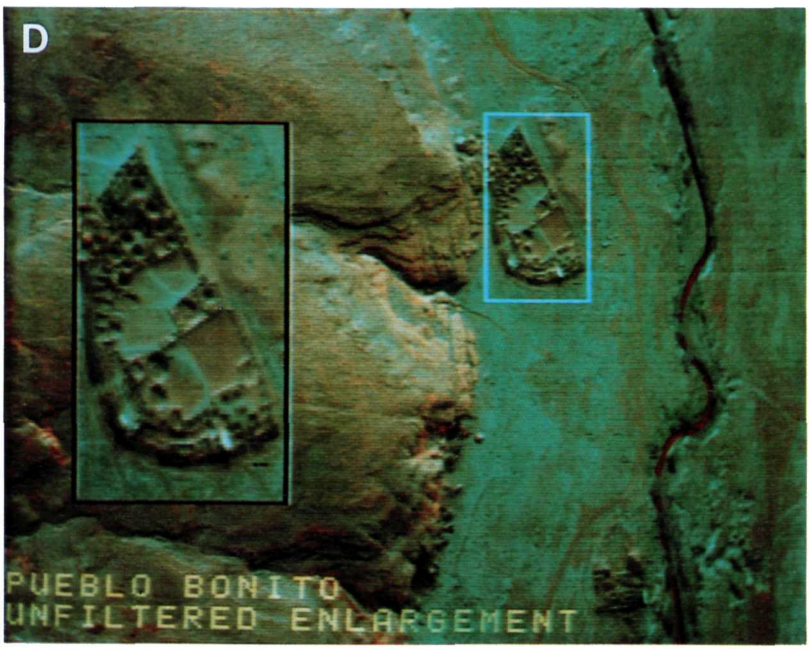

In step 1, an area to to be enlarged is highlighted (shown in orange in fig. 14A). The cursor is then moved off-site, and a block of data space four times its size (2X enlargement) is reserved in the memory module. After this has been accomplished, the enlarged data can be inserted into the reserved space as shown in Figure 14B. Step 3 involves a repeat of steps 1 and 2. The cursor is moved back to the site of interest and carefully positioned to avoid underlap, overlap or sidelap (fig. 14C highlighted in light green). A second block of data space is reserved and the enlargement completed.

The final step in the process involves the placement of boundaries around the areas of interest and labeling. In Figure 14D, we have also added a third channel of data and created a false color composite.

Summary

Table 6 lists the major image processing functions available on the GE Image–100. The system is so flexible that virtually any of the functions can be performed on any set of other functions for anywhere from three to five spectral channels. The studies initiated on Chaco Canyon were purely exploratory and involved only a small fraction of the total data collected. Although we experimented with all of the functional areas, more exhaustive effort needs to be undertaken to fully appreciate which activities are best for archeological phenomena. Figure 15 attempts to capture the breadth of functions available on the Image–100.

The data set obtained by the Bendix M^2S system is considered to be excellent. Ten of the eleven channels were properly functioning and only sporadic scan lines are missing. Channel to channel registration is also the best ever experienced.

Table 6. Image-100 Processing Techniques

Processing Technique	Commonly Performed on:
Scan line clean-up	raw digital data
Contrast stretching 1. linear stretching 2. non-linear (logarithmic or Gaussian)	raw digital data; ratios from raw data
Theme extraction 1. training and alarming 2. 2-dimensional plot and alarming	raw or stretched and/or ratioed, filtered and enlarged image data
Ratioing 1. band ratios 2. multitemporal data	raw or stretched and/or filtered and enlarged image data
Spatial Filtering 1. low pass (smoothing) 2. high pass (edge enhancing)	raw or stretched and/or ratioed image data
Enlargement 1. 2 times 2. 4 times	raw or stretched and/or filtered image data
False Color Composites	up to 4 channels* of raw or stretched, ratioed, filtered and/or enlarged image data

*Usually the 5th channel is reserved for annotation, arrows, highlights, etc.

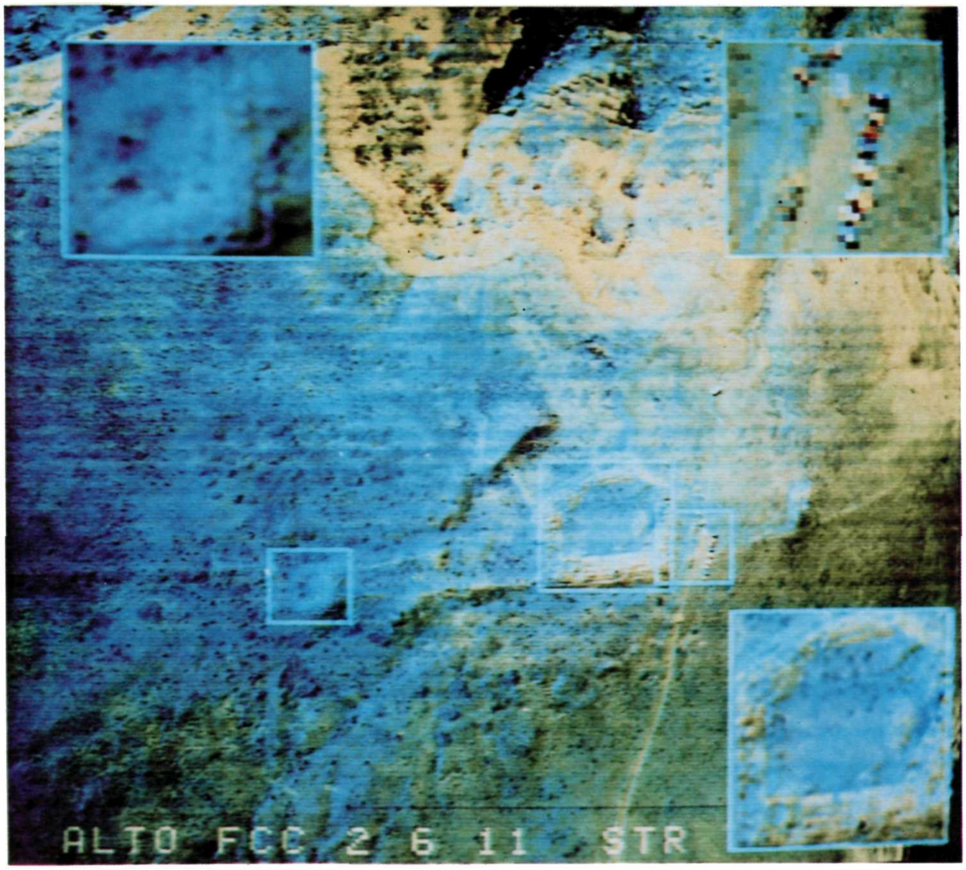

Figure 15 The background image is a linearly stretched false color composite of blue, red-orange and thermal infrared spectral data over Pueblo Alto. Specific sites of interest have been enlarged for easier viewing. Both low pass filtered and unfiltered 2-and 4-time enlargements are shown.

Section 4

Image Interpretation

Several prospects and ideas have been discussed in Part III of this report, but there are specific additional topics that need to be mentioned. For the most part, these focus on locating Anasazi agricultural plots and the prehistoric road net.

Agricultural Fields

As a novice in Anasazi culture, I have struggled with the problem of locating what might have been their agricultural plots. Three confirmed plots have been pointed out to me: one a few feet west of Wijiji, one very large one on the road entering Chetro Ketl, and a small one near Kin Bineola. All three are remarkably, if not perfectly, rectangular and all are obvious, even to the unaided eye. Loose and Lyons (1976) have discussed these and presented sound evidence for about two dozen other sites in the canyon.

An obvious question arises as to why, if the known fields are so clearly visible, are there not more reported occurrences? The answer most often given is that most former fields have been destroyed or buried under several feet of alluvial deposits and sand; or, that they have been eroded completely as the Chaco River became trenched. This argument already explains too much, since the counter question of why these fields, of all those that must have existed, should remain so vivid. Why were they not buried along with all the others? Their specific locations have nothing to recommend their preservation. A related puzzle, and perhaps the key to the problem, is why vegetation regrowth should shun the interiors of confirmed fields even after one to two feet of infilling by sand.

One wonders why there is not a wider range of clearly, moderately and ill-defined fields and field remnants—unless, of course, the aforementioned examples are not Anasazi at all, but of much more recent tillage. Based on the evidence of Loose and Lyons (1976), the fields are probably Anasazi but could still have been titled more recently by later (even modern?) occupants. This might explain both the clarity of field borders and absence of interior vegetation. It might also explain why there appear to be so few field "fragments." The known fields would then be more a result of cultural rejuvenation than environmental inertia. There is, after all, plenty of evidence for modern (last 100–200 years) occupation of the valley, complete with hogans, agricultural fields, and abandoned cultural artifacts. The circular features alluded to in Section III (page 32), might in some cases show the former locations of hogans, and it might be to these that the fields are culturally tied. Figure 16 illustrates one such possibility.

With these observatons in mind, our attempt with the Image–100 was to locate possible prehistoric fields on the Bendix data, but *not* to search for textbook rectangles. At the Pueblo Alto site, we observed an illusively shaped area marked A on Figure 17. In some spectral channels, the area appears rectangular by virtue of its being bounded by clumps of mormon tea, *Ephedra spp.* (fig. 17, upper left). In other channels it assumes more the appearance of a horseshoe (fig. 17, lower left). The accompanying ground photo suggests that the area is not just imagination. It appears that there were low earthen mounds to flood irrigate the site and that the remnants of these mounds are now occupied by mormon tea.

In trying to enhance the feature, we conclude that single bands of raw data portray it about as

Figure 16 Portion of a black and white aerial photograph of the Wijiji site. The areas marked A are suspiciously circular but are too removed from the main site to be kivas. The area at B is reputed to be an Anasazi field. Could it equally be a Navajo garden plot of more recent origin or an Anasazi field rejuvenated by more cultivation?

well as any other technique—at least for those spectral data we studied. Neither contrast stretching, band ratioing, color compositing or feature extraction significantly improved its detectability.

At Kin Bineola, we also searched for agricultural fields; but, unlike the case at Pueblo Alto, we believe that band ratioing showed more than raw data. Figure 18 is a rather encouraging result after an admittedly brief look. The image is a tri-ratio color composite created by ratioing channels 2÷6 and displaying the result in green; 6÷8 displayed in blue; and 8÷11 in red. Other, more pleasing, color combinations were reviewed, but none enhanced the pattern as well as the one shown. Arrows were included at the time to pinpoint rectilinearities, right angles and other straight-line segments that might relate to an old field system.

It is reasonable to hypothesize an old system at this general locale because of the more or less dense drainage net which might have provided a source of irrigation water over a large hinterland catchment. No field verifications have been made. We strongly recommend that all the data be systemmatically reviewed for rectilinearities and other evidence for past agricultural activity.

Buried Structures

For Chetro Ketl, a case has already been made for the possible "discovery" of a kiva system and buried walls in the discussion relating to Figure 8. If these kivas really exist, their appearance on the imagery is most likely due to soil moisture differences. Following the strategy discussed in Figure 11, such differences might be enhanced further by band ratioing. We therefore recommend that additional work be undertaken to verify this approach and to extend the analysis not only to other known sites but throughout the area covered by the multispectral data.

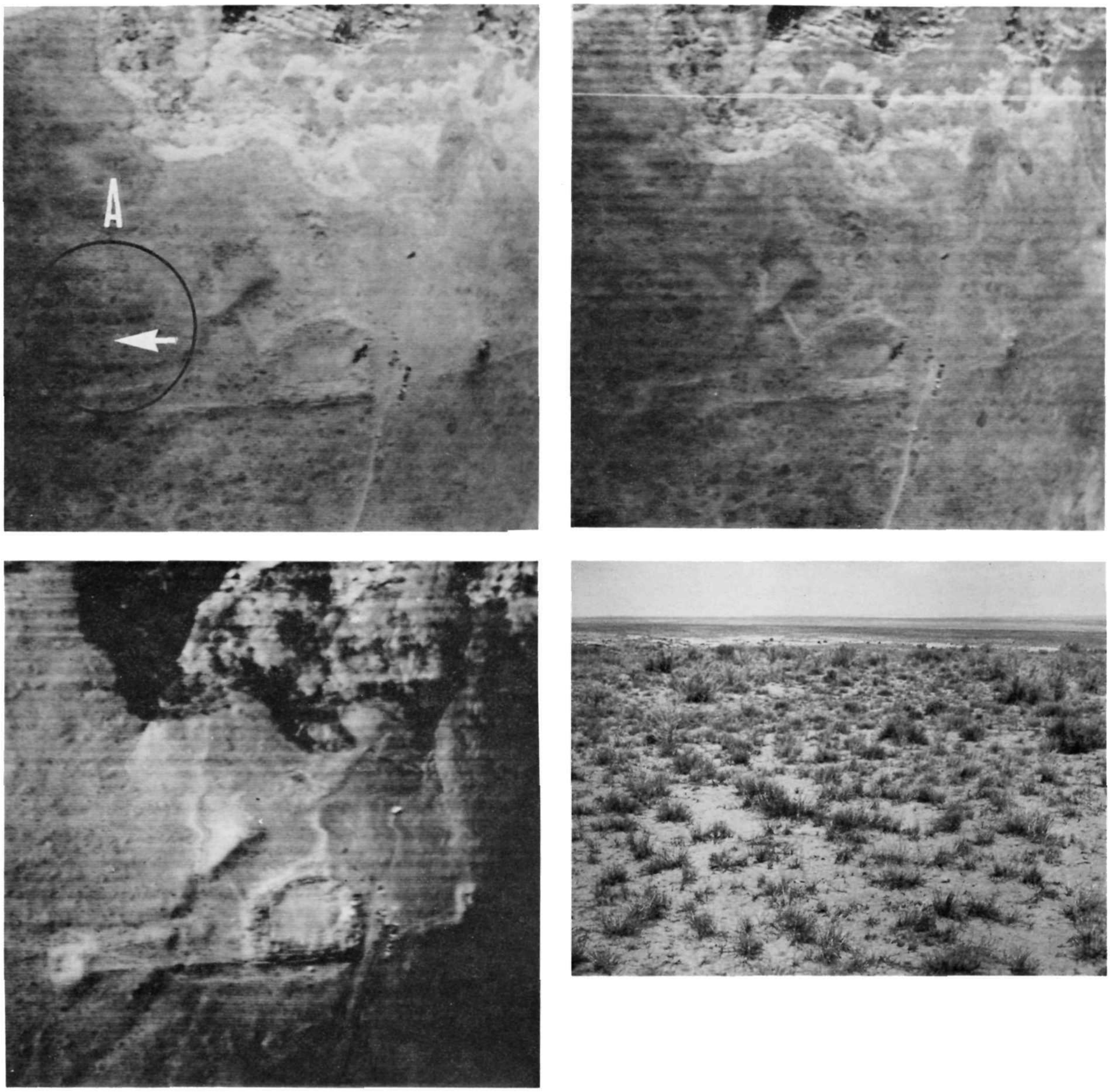

Figure 17 Sequence of Bendix spectral data showing variable appearance of a possible old field (A). Upper left is reflective infrared (Channel 10 linearly stretched): upper right is reflective infrared (Channel 8 raw data); lower left is thermal infrared (Channel 11 linearly stretched); lower right is a field photo looking in the direction of the arrow.

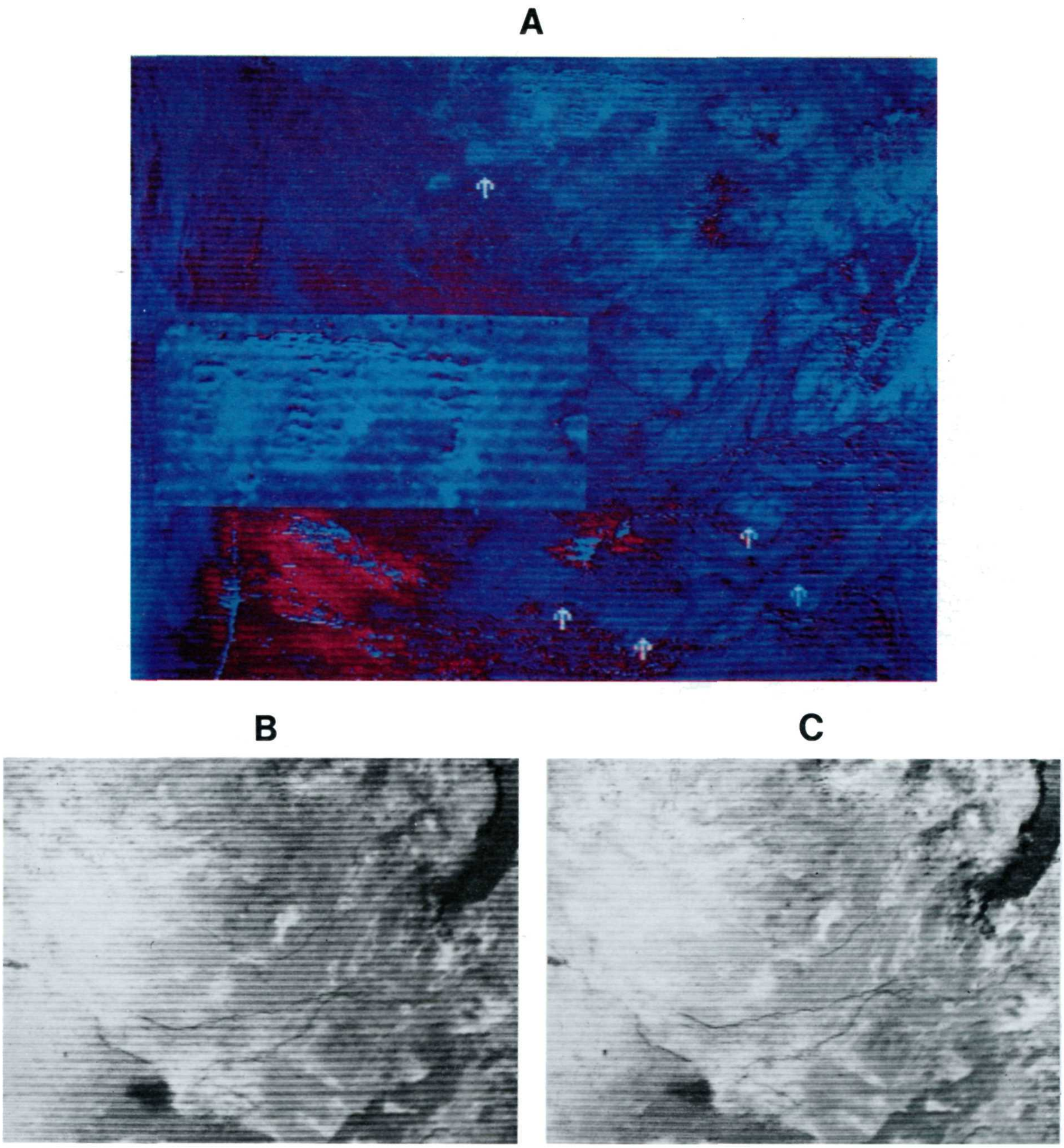

Figure 18 Tri-ratio color composite of the Kin Bineola region. A possible field system is indicated by a series of arrows. The arrow at the top points to an area often reported as a prehistoric field. B and C are raw data for Channels 2 and 8 respectively. Our opinion is that they do not reveal the pattern as well as the ratioed image.

Another attribute of the data that should be thoroughly reviewed is the psuedo-relief models portrayed in combinations involving the thermal channel. In Figure 19 of Pueblo Alto, for example, the more or less raised feature indicated at A could be culturally related. The structures at B, C, and D of course are well known, as are the walls connecting them. There are also indications of a wall at E between A and B, and if this exists, there would be added credence for a structure at A. Across track siting at ground level from B to A and D to A fails to reveal any evidence for even a slightly raised feature.

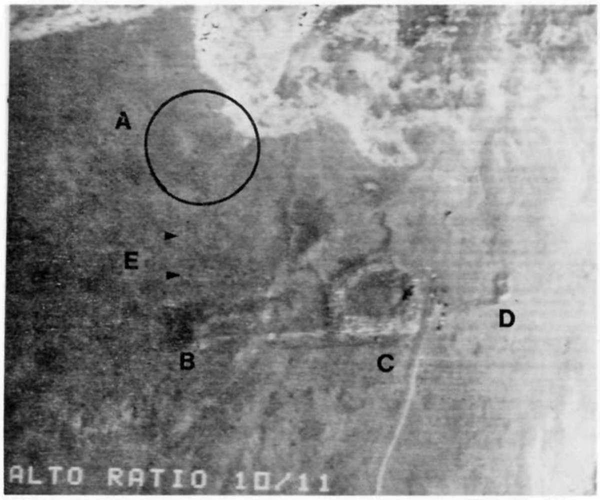

Figure 19 Location of a possible culturally related feature (A) with a connecting wall (E) at Pueblo Alto.

Prehistoric Roads

The discovery of additional roads on the prehistoric net was not an objective of this analysis. We felt this aspect of the canyon's cultural pattern was already fairly well known and reported. A segment of the road leading from Chetro Ketl to Pueblo Alto was discussed in Figure 8. In Figure 20A there is evidence for three roads radiating northward out of the gate at Pueblo Alto. There are several confirmed prehistoric roads reported for the area, as shown in Figure 20B. The only difference is that the angles of radiation out of the gate appear to be somewhat different from those shown on the map.

One of the analyses not conducted for the study was high-pass filtering, or edge enhancement. In view of the fine spectral and spatial resolution of the data, we suggest that additional road confirmations might be possible through high-pass spatial filter analysis.

A

B

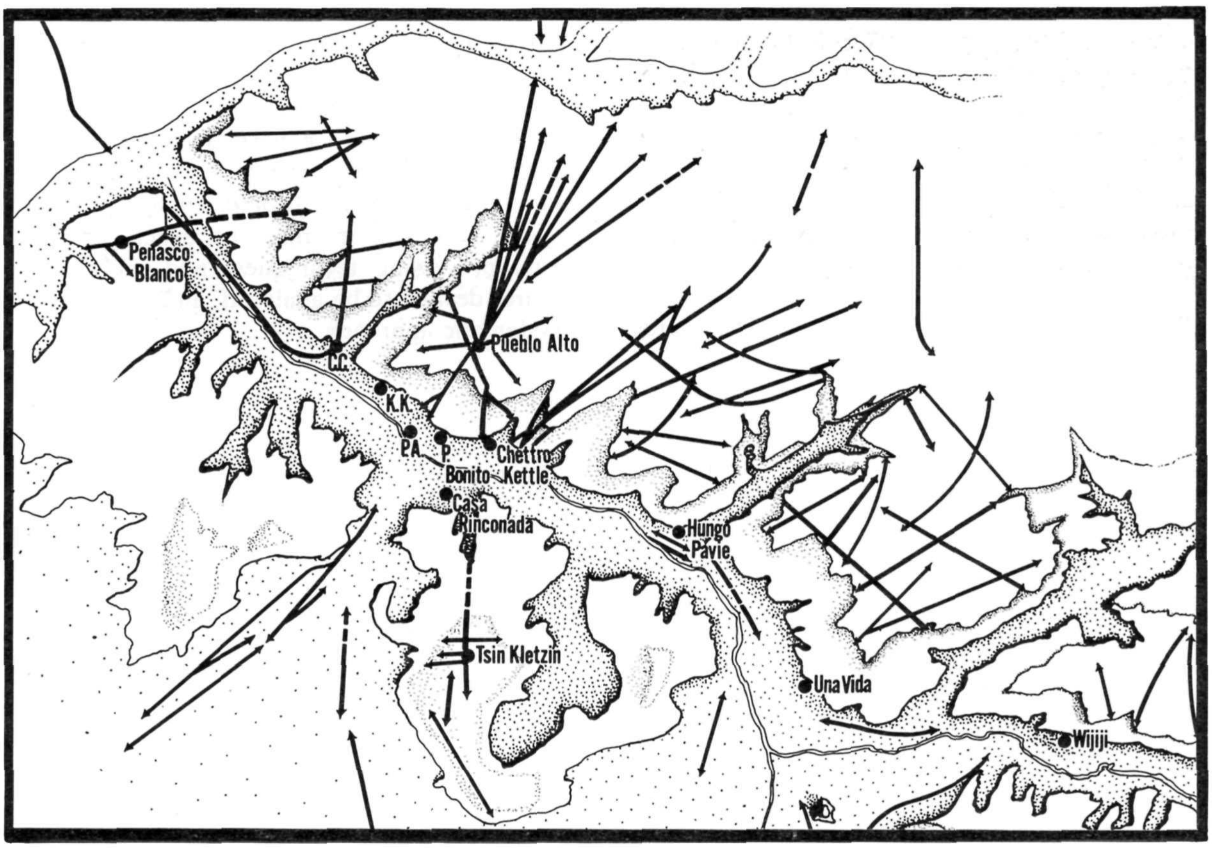

Figure 20 A reflective infrared image (A) of Pueblo Alto showing 3 prehistoric roads radiating from "the north gate." The angles of radiation differ slightly from those confirmed roads shown in the map (B).

Section 5

Conclusions

The multispectral analysis techniques described here show great promise for assisting field archeologists in their search for agricultural patterns, structures, and transportation links. Although our studies were severely limited in geographic coverage, the various results from Pueblo Alto, Chetro Ketl, and Kin Bineola argue strongly for continuation of the analysis effort.

The soil moisture and vegetation density correlations proved of limited value. The landscapes studied were virtually isomorphous and isothermic with only broad distinctions being possible between the riparian forest along the Chaco River, the Chaco Valley itself, and the uplands. The average sample-to-sample surface moisture differences along the transects at Pueblo Alto and Kin Bineola were so small that they translated into negligible thermal differences. Thermal patterns are observable on the Channel 11 image at Kin Bineola because of vegetational effects, but vegetation *density* does not seem to be the key parameter.

For subsequent analysis, we suggest that a matrix table similar to that given here be created and a strategy developed *before* image processing begins. This will optimize the exact geographic areas, processing techniques, and archeological features desired to be analyzed, and should ensure a systematic approach.

References

ANDERSON, D. AND B. ANDERSON
1976 *Chaco Canyon*, Southwest Parks and Monuments Association, Globe, Arizona. Popular Series No. 17, 50pp.

BENDIX CORPORATION
1975 *M^2S: Modular Multispectral Scanner-System Description*, BSR4167A, Ann Arbor, Michigan.

GOUREVITCH, A.
1963 *Soil-Geographical Zoning of the U.S.S.R.*, Israel Program for Scientific Translations, Jerusalem, 480pp.

LOOSE, R.W. AND T.R. LYONS
1976 "The Chetro Ketl Field: A Planned Water Control System in Chaco Canyon." In *Remote Sensing Experiments in Cultural Resource Studies—Non-destructive Methods of Archeological Exploration, Survey, and Anaylsis*. Reports of the Chaco Center #1. National Park Service and University of New Mexico. pp. 133–156.

APPENDIX A

% Moisture

(Refer to Figure 2 for location of each transect)

Pueblo Alto Transect A

	S	D
A1	6.02	2.52
A2	4.85	2.80
A3	ND	ND
A4	6.67	2.89
A5	3.14	2.07
A6	4.19	2.99
A7	6.70	2.86
A8	7.06	4.45
A9	5.01	2.02
A10	5.55	3.64
A11	4.73	1.40

Pueblo Alto Transect B

	S	D
B1	4.88	2.34
B2	4.89	1.86
B3	5.61	2.49
B4	4.95	0.74
B5	4.19	1.97
B6	3.87	4.51
B7	3.72	2.53

Pueblo Alto Transect C

	S	D
C1	5.10	2.99
C2	5.24	5.31
C3	3.74	2.39
C4	4.52	2.97
C5	4.50	2.36
C6	5.03	4.90
C7	4.98	3.01
C8	4.33	1.80
C9	4.62	2.54
C10	3.68	2.32
C11	4.32	3.92
C12	3.55	2.79

Pueblo Alto Transect D

	S	D
D1	6.31	2.52
D2	5.20	2.20
D3	5.24	2.07
D4	5.60	1.94
D5	6.79	3.15
D6	6.02	5.33
D7	4.14	2.57

Pueblo Alto Transect E

	S	D
E1	8.63	0.55
E2	8.16	1.65
E3	7.38	0.99
*E4	8.32	2.47
*E5	8.81	2.72

Pueblo Alto Transect F

	S	D
F1	6.56	2.09
F2	6.64	1.48
F3	7.51	2.06
F4	8.28	1.39

Pueblo Alto Transect G

	S	D
G1	3.03	2.01
G2	4.16	3.11
G3	4.13	2.37
G4	3.22	2.25
G5	3.45	3.21
G6	2.61	1.38

Pueblo Alto Transect H

	S	D
H1	3.94	1.41
H2	7.03	12.81
H3	3.82	3.73
H4	3.26	2.76
H5	2.98	2.98
H6	2.37	2.18

Pueblo Alto Transect I

	S	D
I1	5.35	1.92
I2	7.73	1.64
I3	7.73	1.59

Kin Bineola Transect A

	S	D
A1	4.43	1.92
A2	3.65	1.82
A3	2.23	1.50
A4	3.76	4.53
A5	2.84	2.31
A6	4.39	1.80

Kin Bineola Transect B

	S	D
B1	5.36	4.52
B2	6.11	3.04
B3	5.78	4.78

Kin Bineola Transect C

	S	D
C1	6.85	2.28
C2	5.61	2.61
C3	3.82	0.83
C4	3.93	0.93
C5	1.69	1.51

Kin Bineola Transect D

	S	D
D1	2.97	1.41
D2	4.40	0.76
D3	4.70	4.41
D4	5.50	10.10

Kin Bineola Transect E

	S	D
E1	7.00	6.61
E2	8.17	20.0

Kin Bineola Transect F

	S	D
F1	5.01	7.62
F2	5.05	5.28
F3	2.93	4.60
F4	3.72	5.78
F5	3.69	7.37

Kin Bineola Transect G

	S	D
G1	5.30	6.84
G2	3.10	3.03
G3	4.66	1.49
G4	5.65	6.69

Kin Bineola Transect H

	S	D
H1	2.61	1.79
H2	5.60	2.25
H3	2.90	1.30

Wijiji Transect A

	S	D
A1	1.12	0.46
A2	0.98	0.88
A3	0.97	1.14
A4	1.34	0.87
A5	3.22	4.48
A6	3.64	4.63
A7	3.63	5.77
A8	2.07	4.43
A9	0.79	1.03
A10	1.17	0.94

Wijiji Transect B

	S	D
B1	2.78	5.26
B2	2.94	4.91
B3	2.43	4.37
B4	3.48	6.76
B5	2.37	3.14

* D samples for E 4&5 *may* have been reversed

PART 2

Remote Detection of Prehistoric Sites in Bandelier National Monument

Stanley A. Morain
Charles Nelson
Mike E. White
Amelia M. Komarek

Contents

Illustrations

Tables

Acknowledgments

Analytical procedures for this report were performed in the Data Analysis Laboratory, Earth Resources Observation Systems (EROS) Data Center, Sioux Falls, SD. Technology Application Center (TAC) and the National Park Service wish to acknowledge the assistance provided by personnel in the Lab for giving so freely of their time and experience. The analyses could not have been performed without their aid.

Section 1

Introduction

Background

In October, 1976, the National Park Service, Office of Contract Archeology, arranged for a Bendix* 11-channel M^2S scanner to be flown over several archeological areas in New Mexico. Their purpose was to evaluate airborne spectral data as a means for non-destructive exploration of Anasazi and pueblo cultural sites in Chaco, Cochiti and Garcia Canyons, and Bandelier National Monument. In a previous paper, Morain et al. (1977) presented an analysis of the Chaco Canyon data. That report focused on image processing techniques to enhance such features as prehistoric agricultural fields, anthropogenic soil patterns, buried walls and kivas, and prehistoric road traces. It was essentially a description of the range of enhancement capabilities using a hard-wired General Electric Image 100—system+. The analyses included contrast stretching, band ratioing, high and low band-pass filtering, color compositing and single class color enhancing. The EROS Data Center provided the system and expertise for its use as part of their charter for support of Department of Interior demonstration projects.

From the experience gained at Chaco Canyon, a follow-on experiment was undertaken to assess prehistoric sites at Bandelier National Monument. The aim of this effort was to subject the multispectral scanner data (MSS) to both supervised and unsupervised enhancement/classification techniques in a further test of image analysis for cultural information. Principal components and canonical analyses were performed on an identical 512 scan line × 512 sample data matrix. Since each resolution cell (pixel) was about 3.75 feet (1.25 m) square, the subscene covered an area of about 1920 feet (585 m) on a side (0.13 sq. mi. or .34 sq. km.). Within this area several prehistoric sites were known to exist by virtue of their annotation on the USGS 1:24,000 Frijoles quadrangle.

*Early in 1978 the Bendix Aerospace Division at Ann Arbor was acquired by the Environmental Research Institute of Michigan (ERIM).

†The use of trade, firm, or corporation names in this Publication is for the information and convenience of the reader. Such use does not constitute an official endorsement or approval by the U.S. Department of the Interior of any product or service to the exclusion of others that may be suitable.

Problem Statement

The basic study question was whether the enhancement/classification techniques were capable of spectrally enchancing known prehistoric sites from surrounding terrain. Equally important was the need to know whether additional, unmapped sites might be revealed through these techniques. Analytically, there was interest in discovering whether the unsupervised or supervised technique yielded more readily interpretable results. The intent of the investigation was more sophisticated than that performed at Chaco Canyon in that the procedures were based on statistical grouping techniques and probabilities rather than algebraic manipulation of pixel digital counts.

The reason for using more involved algorithms to analyze the environment at Bandelier National Monument is partly because of the subtle expression of features under study. The site plotted on the U.S.G.S. topographic quadrangle maps are labeled as "ruins". This suggests that either there are exposed remains of structures or there are indications of buried foundations, walls or complexes. It is known, however, that human occupancy at Bandelier included a range of activities, only a few of which resulted in lasting structures or their ruins. It is important to note, however, that our procedures and results apply to all human impacts, not only structures. Our hypothesis was that human disturbance of the environment could be detected through spectral analysis. In order to be detected, such disturbance would have to have been localized or prolonged, or brief but very intense. In terms of remote sensing, this problem is not dissimilar to that in agriculture and forestry where stress and pest infestations must be locally intense to be spectrally identifiable using systems with relatively coarse spatial resolution. An adverse consequence of this approach to classification is that, if intensely disturbed sites were detected, there would be no *a priori* knowledge as to the nature of the disturbance. Consequently, field checking would be required to determine the archeological significance of these prehistoric sites.

The Physical Environment

Bandelier National Monument is located near Los Alamos in the Jemez Mountains of north-central New Mexico (fig. 1). Tourists to the area are familiar with the extensive ruin complexes in Frijoles Canyon where the Monument headquarters are located (fig. 2). However, on the mesas between Frijoles, Alamo, and Capulin Canyons, west of the headquarters, there are hundreds of local and much less spectacular archeological sites. Aside from Monument personnel, only a few determined backpackers ever see these, because the area is closely protected by park personnel, and the canyons have exceedingly steep walls that impede access. Figure 3 is part of the Frijoles quadrangle (7½-minute topographic map) showing the general location of Bandelier Monument headquarters and the location for the present study.

The mesas southeast of the Jemez Caldera are formed from thick deposits of volcanic tuff and ash blown from the Jemez volcano during Pleistocene and Recent geologic time. These materials are relatively soft and porous, and consequently, they have been dissected by steep canyons. Soil development and organic build-up on the surface has been negligible and the related high background albedo is therefore attributed to the tuff itself.

Precipitation in the region averages sixteen inches (400 mm) per annum. The porous nature of the bedrock combined with high evapo-transpiration (summer high temperatures exceed 80° F or 23° C) results in a low soil moisture content. Throughout the mesa/canyon complex below about 6500 feet, the vegetation consists of piñon-juniper (*Pinus edulis—Juniperus spp.*) woodlands with occasional ponderosa pine (*Pinus ponderosa*) and small grassy clearings. Total cover of the overstory trees, as interpreted from a crown density scale from 1975 Forest Service photography, averages less than 35–45 percent. Forest tree species tend to be found in patches or clusters. Vegetative ground cover is equally open, if not more sparse. Along the upland drainage lines, and in swales, one can find local concentrations of great basin sage (*Artemisia tridentata*) and rubber rabbit brush (*Chrysothamnus spp.*). These stands tend to be somewhat more dense and in some cases may approach complete cover.

Site Variability

A field visit to about one dozen cultural sites southeast of the Monument headquarters was made prior to data analysis. The sites provided a basis for describing the range of variability of prehistoric sites in the study area. The places visited included Frijolito, one of the few named ruins, and a series of easily accessible but subtle, unmarked sites. Figure 4 shows the field views of some of these sites. These localities are identifiable by the presence of small potsherds usually around a small mound and a few building stones, but otherwise they look like the surrounding countryside. In the larger and more visible sites, partially excavated wall structures were seen.

From the field observations, it was estimated that the most intensely disturbed sites range in diameter from 25 to 40 feet (7.6-12.2 m). With the given resolution of 3.75 square feet, our analysis for any given site involved anywhere from 30 to 90 independent spectral samples (pixels). Although the smaller sites were close to the lower limit of statistical reliability for sample size, the larger sites were well above that limit.

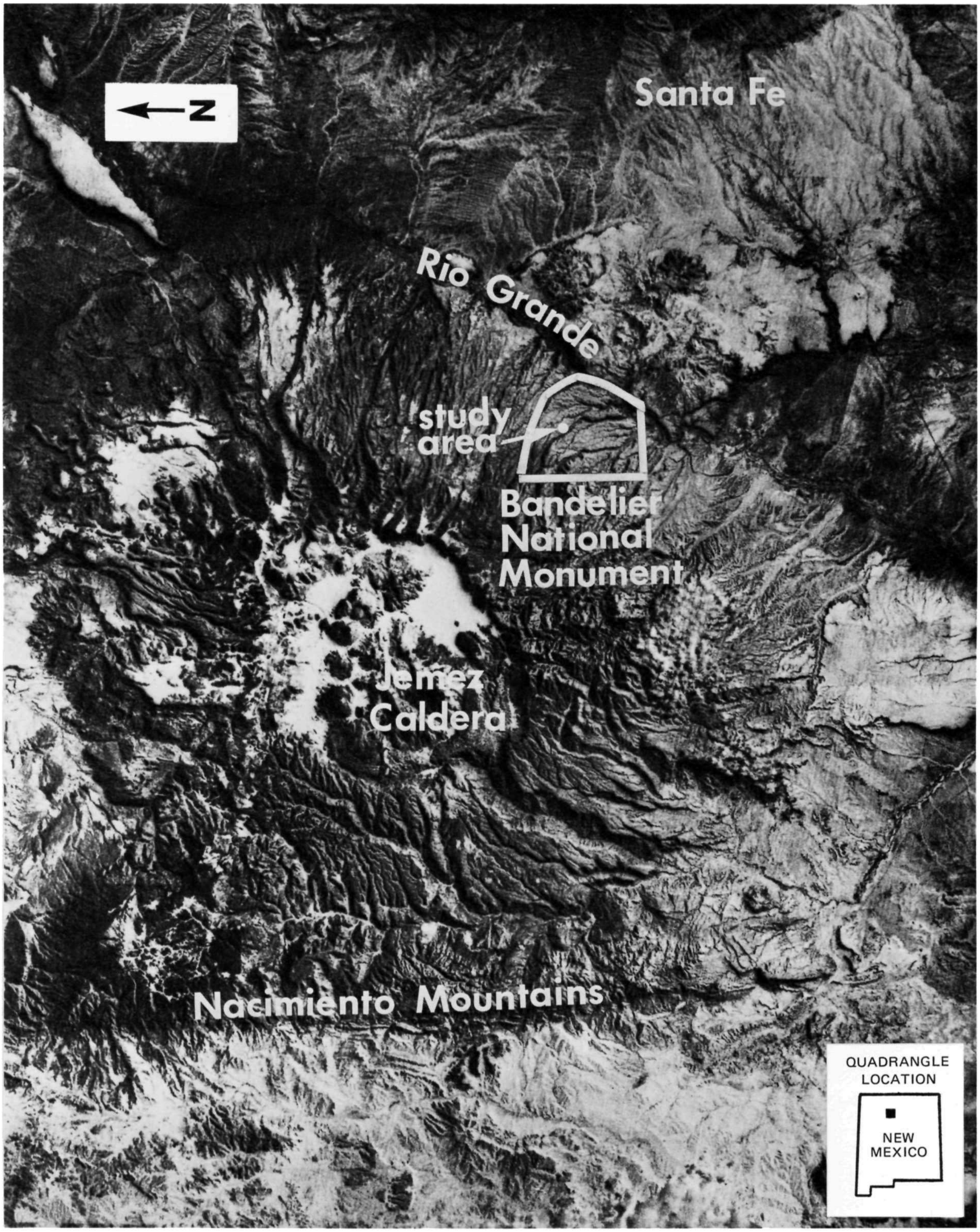

Figure 1 Location of Bandelier National Monument. Scale—1:500,000 Landsat Image 1460–17125

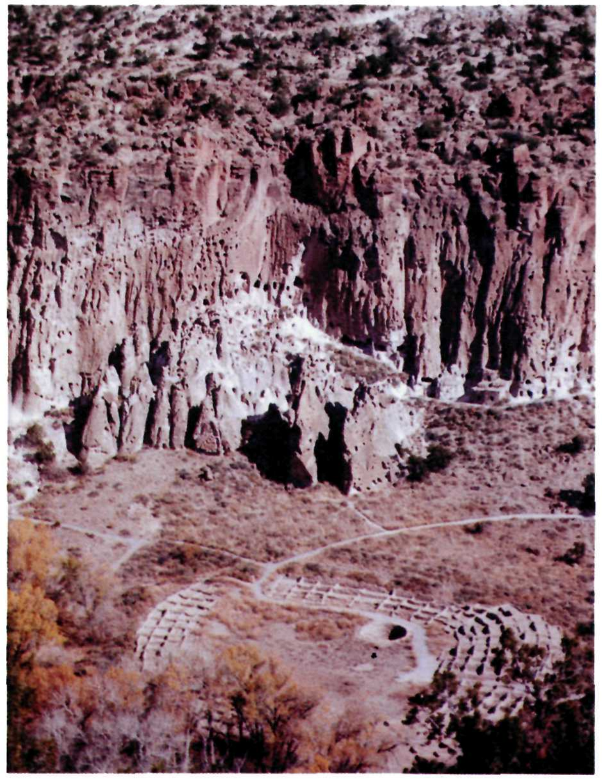

Figure 2 (Above) Tyuonyi Ruins in Frijoles Canyon are one of the most impressive sites in the Rio Grande drainage. These ruins are the closest to Bandelier headquarters and are among the most frequently visited of the ancient pueblo ruins.

Figure 3 (Right) Location of study site in Bandelier National Monument.

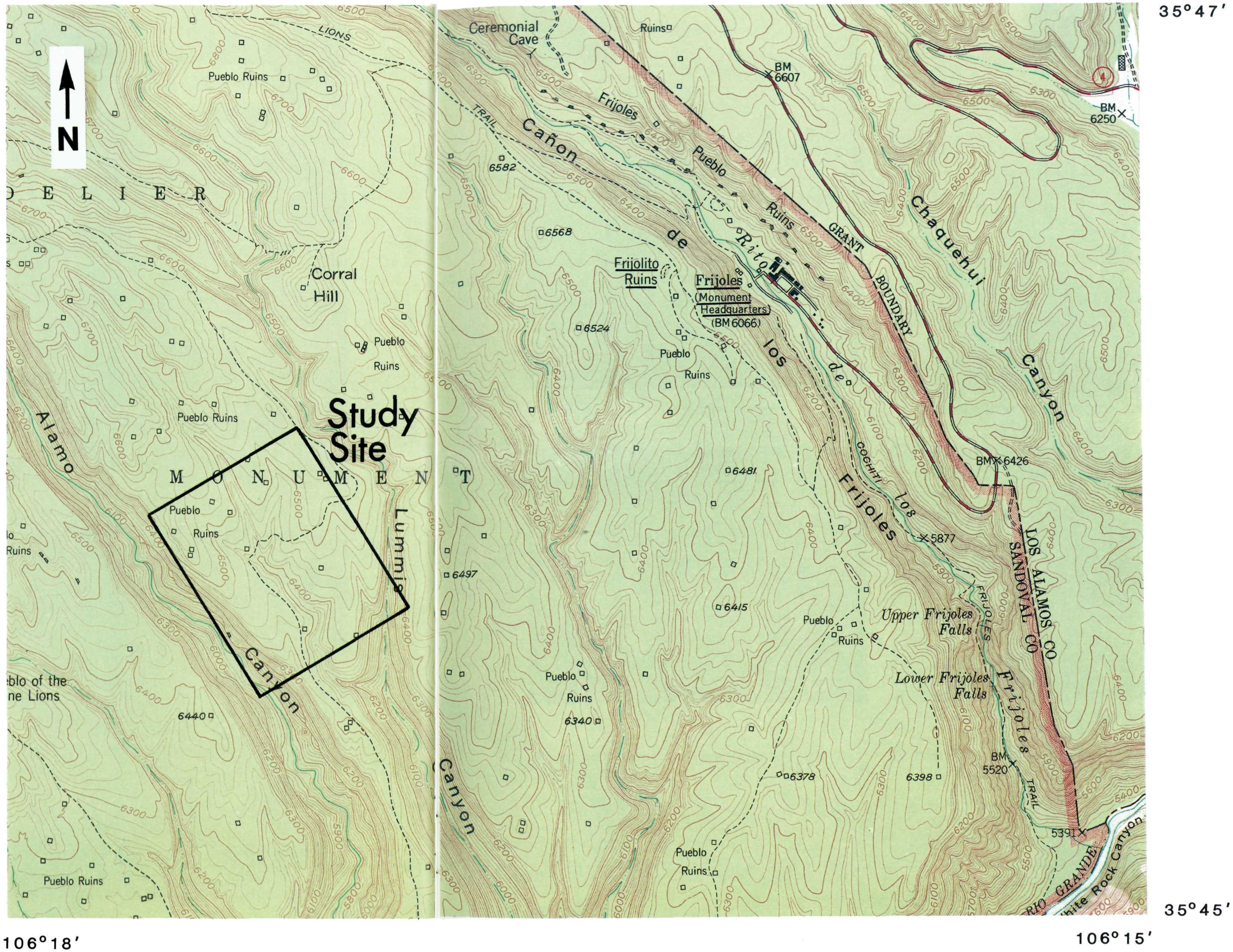

Frijoles, New Mexico
Scale – 1:24,000

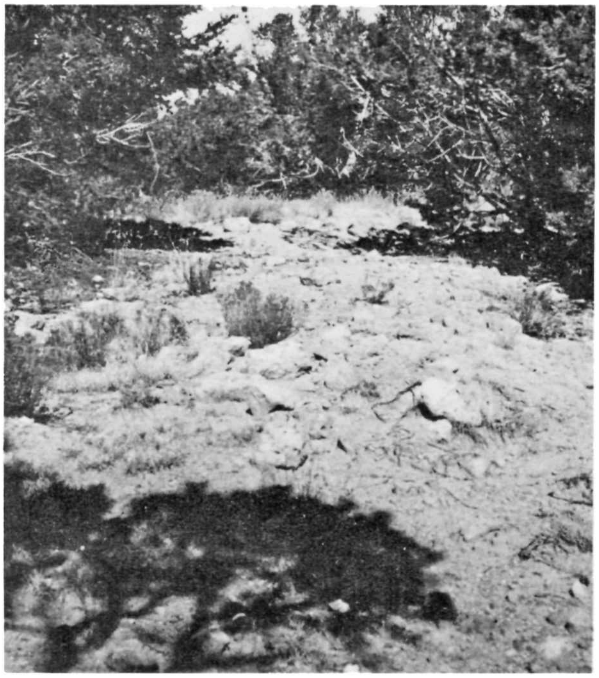

Prehistoric site without wall remnant

Ruin

Prehistoric site without wall remnant

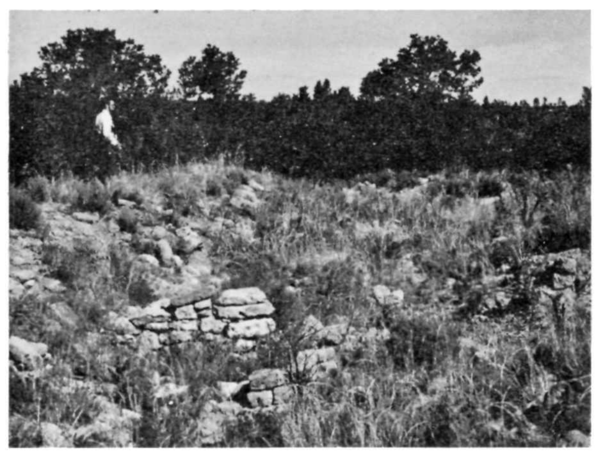

Ruin

Figure 4 Typical views of prehistoric sites on the mesa west of Frijolito Canyon. Note the sparse vegetation and high surface albedo.

Three items regarding the spectral and spatial appearance of disturbed sites should be noted. First, it was observed that few sites are inhabited by either piñon and/or juniper. Sites generally have a sparse cover of bunch grass or are essentially barren. Therefore, one could anticipate difficulty in trying to distinguish such areas from natural terrain classes called "grass" or "bare soil." Second, sites are sometimes ringed by piñon and/or juniper. In this condition, their photomorphic signature may be contrasted against their background, but not particularly distinguishable through current image processing strategies that use only spectral properties as variables. Third, disturbed sites located on ridges or low drainage divides often have remnants of walls or other structures. It is assumed that these were dwellings located on somewhat higher ground for reasons of protection. Sites located off the higher ground may have been used for other purposes.

Section 2

Methodology

Morain et al. (1977) have described the Bendix data characteristics in detail. A summary of the sensor specifications compared to other MSS systems is given in Appendix A. The M^2S scanner operates to collect data with wavelengths ranging from ultraviolet to thermal infrared. At the time of data acquisition, the ultraviolet channel was not fully functional, so only 10 channels of usable data were acquired in the .38 to 12.25 wavelength range. The wavelengths of these channels are shown in Appendix B. The system has a 2.5 milliradian field of view and was flown at 1500 feet (457 m) to provide a ground resolution of 3.75 square feet (1.25 m^2). The data used in our assessment of prehistoric sites consisted, therefore, of a 10 element vector for each 3.75 feet by 3.75 feet piece of terrain.

Two enhancement algorithms and a maximum likelihood classifier were used in the analysis. The principal components algorithm was used to see if an "unsupervised" enhancement would spectrally enhance prehistoric sites without *a priori* knowledge or without making any assumptions about the landscape. If they could be discriminated, this fact would be strong evidence that these occupation sites inherited long lasting spectral attributes arising from the disturbance of the original physical/biological characteristics of the site. Enhancement of these spectral attributes would allow an archeologist to better discriminate anomalous spatial relationships that may be interpreted as archeologically significant patterns. This experiment with principal components is viewed as a test of the null hypothesis that *prehistoric sites cannot be visually discriminated by spectral properties alone.*

The second enhancement algorithm, canonical analysis, is described as "supervised" because spectral signatures from known sites are used to enhance the variability among spectral classes and reduce the variability within a class. Again, our desire was to determine if prehistoric sites were spectrally discriminable. But, in this case, the analysis was assisted by looking at the spectral responses of known sites and enhancing their spectral separation over the rest of the study area. Our null hypothesis was that *prehistoric sites, even if ground data is used to direct the enhancement, cannot be visually discriminated by spectral properties alone.*

A maximum likelihood classifier using the "supervised" training approach was also used for testing the second hypothesis. This approach used the same sample sites as the canonical analysis, but instead of enhancing the data, it created a new image where each picture element was statistically assigned to a spectral class representing a resource type determined in training.

Principal Components Analysis

The principal components analysis is a technique for transforming multivariate data into a series of uncorrelated axes. Each of the ten spectral channels is an axis of variability. The data are transformed to describe the same total variance with the same number of variables, but in such a way that the first axis accounts for as much of the total variance as possible, the second axis accounts for as much of the remaining variance as possible while being independent of the variability expressed along the first axis; and so on. Normally, for data that are correlated in their raw form, this results in the data being represented on a few axes which account for most of the total variance and a larger number of small axes that account for very little of the total variance. Usually, the smaller axes can be discounted from further consideration, but sometimes they reveal interesting multispectral attributes in the original data.

Because of the large number of data values, it was unwieldy to work with the entire data set to compute the variance/covariance matrix. In our case, there were 512 × 512 resolution elements (Pixels) in each of 10 variables, one for each spectral channel. In order to conduct an analysis without introducing bias, we selected a 20 percent random sample of the pixels.

Table 1 shows the total amount of variation "explained" by each of the axes resulting from this analysis. The compilation indicates that the first three axes account for more than 96 percent of the variation in the spectra. The question as to how much each spectral channel contributed to each axis is answered by the component loadings as given in Table 2. High positive and negative values indicate the original spectral bands which contribute most to each axis. For the first axis all spectral channels seem to be important. The reflective infrared channels are loaded heavily as an inverse function along the second axis indicating that their responses are different from the other channels after the brightness component (axis 1) has been removed. Importance of the thermal infrared channel decreases after the third axis.

Using the principal component images (fig. 5) as input to standard color enhancement procedures, color composite images were produced. For example, Figure 6 is a composite of component numbers 1, 4, and 5 displayed in blue, green, and reds respectively. Individual trees and open areas can be discerned; the latter, in particular, shows as a spectrum of colors. When comparing this combination of components and color patterns with known locations for prehistoric sites, no correlations could be made. No other combination of three

Table 1: Percentage of Variability Contributed by Each Principal Axis

Axis	1	2	3	4	5	6	7	8	9	10
% "Explained" Variability	78.76	11.34	6.18	1.58	1.01	.42	.29	.21	.14	.07
Cumulative %	78.76	90.10	96.28	97.86	98.87	99.29	99.57	99.79	99.93	100.00

Table 2: Component loadings.

Axis Channel	λ (*nm*)	*Color*	1	2	3	4	5	6	7	8	9	10
1	465	blue	.3548	.2632	.4353	−.4474	−.6180	.0469	.0347	.1398	−.0971	.0305
2	515	green	.3156	.1418	.2154	.3481	−.0543	−.6460	−.1142	−.3253	.4160	−.0221
3	560	yellow green	.3111	.0693	.2003	−.0164	.2935	.3857	−.1106	−.6406	−.2232	.3881
4	600	orange	.2793	.1611	.1825	.3715	.2049	−.0870	.0324	.1835	−.6528	−.4629
5	640	red orange	.2491	.1239	.1674	−.1279	.3516	.4171	.1138	.0842	.5530	−.5047
6	680	red	.2416	.1245	.1048	.2373	.2477	.0074	.3631	.5372	.1169	.6027
7	720	reflective IR	.2409	−.2144	.0116	−.2130	.2406	−.0941	−.8054	.3534	.0084	.1004
8	815	reflective IR	.3577	−.5675	−.1152	.4613	−.4369	.3491	−.0290	.0259	.0911	−.0360
9	1015	reflective IR	.3695	−.5206	−.1441	−.4544	.2094	−.3444	.4197	−.0933	−.1167	−.0656
10	1100	thermal IR	.3958	.4582	−.7858	−.0534	−.0977	.0275	−.0447	−.0244	−.0067	−.0061

* These values indicate the relative importance of each spectral channel in contributing toward the percentage of variability accounted for by each axis.

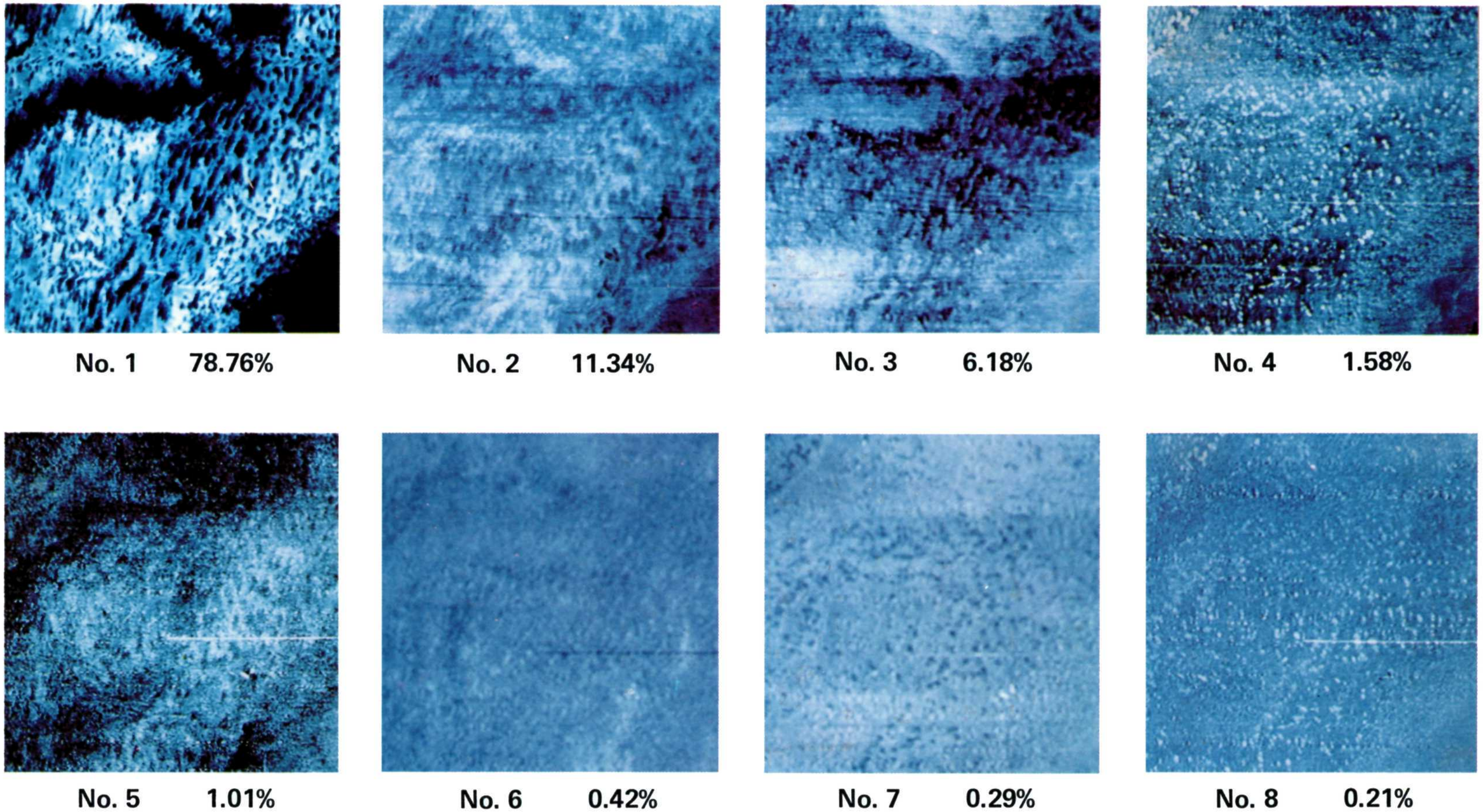

Figure 5 Principal Components images show how the amount of variability (number of grey tones) and precentage contributed decreased as the number of the component gets larger.

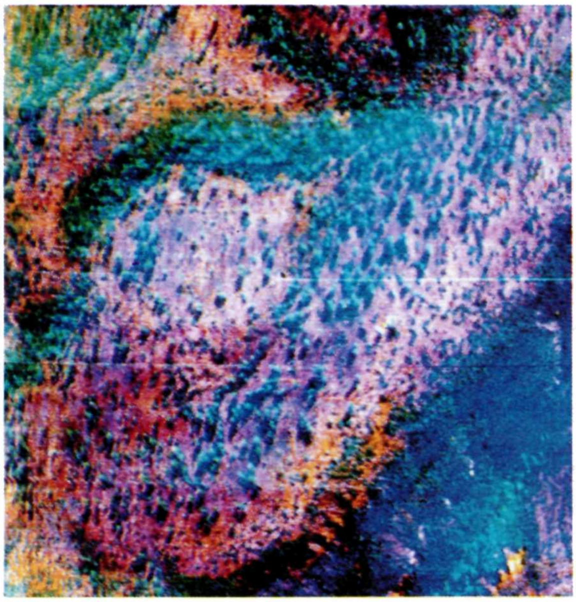

Figure 6 Color composites of Components 1, 4 and 5 displayed in blue, green and red respectively. Though colorful, the image fails to provide useful information on prehistoric sites.

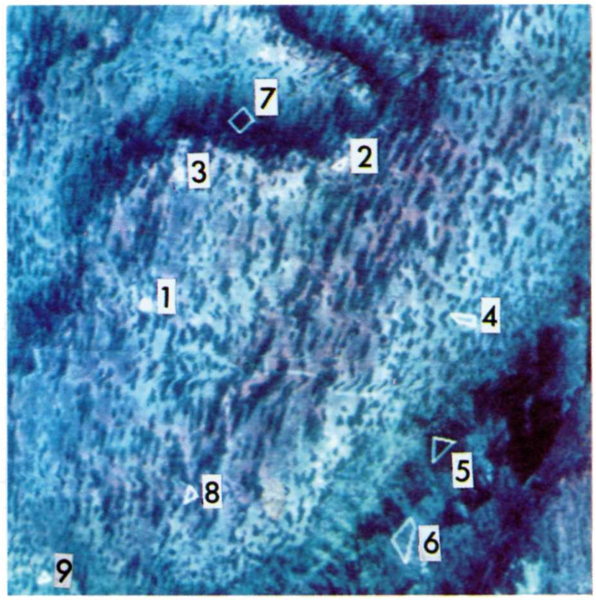

Figure 7 Nine training areas were chosen by using an electronic cursor to delineate terrain classes. Numbers 1, 2, 3, 4 are culturally disturbed site; 5 is defined as "cliff"; 6 is "bare soil"; 7 and 8 are "tree" types; and 9 is "grass." Site 2 had the smallest number of pixels (25); and site 6 had the largest (337). The average number was 118 pixels.

components gave a more interpretable image than that shown in Figure 6. Based on this observation, our conclusion is that the null hypothesis cannot be rejected.

Canonical Analysis

An alternative to the "unsupervised" random sampling of a data set is to pre-define "supervised" classes that will be used to drive an enhancement. Canonical analysis uses the statistical means and covariance of close selected classes to determine coefficient loadings which will increase the variance among classes while decreasing the variance within classes.

In this analysis, nine areas were used as training sites (fig. 7). Four of these were chosen because they coincided with plotted positions for cultural sites on the Frijoles quadrangle. In addition, two types of tree categories were delineated and one each for "cliff," "bare soil," and "grass."

The data were transformed by canonical analysis into a series of uncorrelated axes in such a way as to maximize the variance among the classes and minimize the variance within each class. Eight of the ten canonical axes were used; the remaining two accounted for so little variance that they were considered to be meaningless. Table 3 gives the percentages.

Table 3. Percentage of Variability Contributed by Each Canonical Axis

Axis	1	2	3	4	5	6	7	8
% "Explained" Variability	72.17	19.9	3.61	3.09	.76	.26	.19	.01
Cumulative %	72.17	92.07	95.68	98.77	99.53	99.79	99.98	99.99

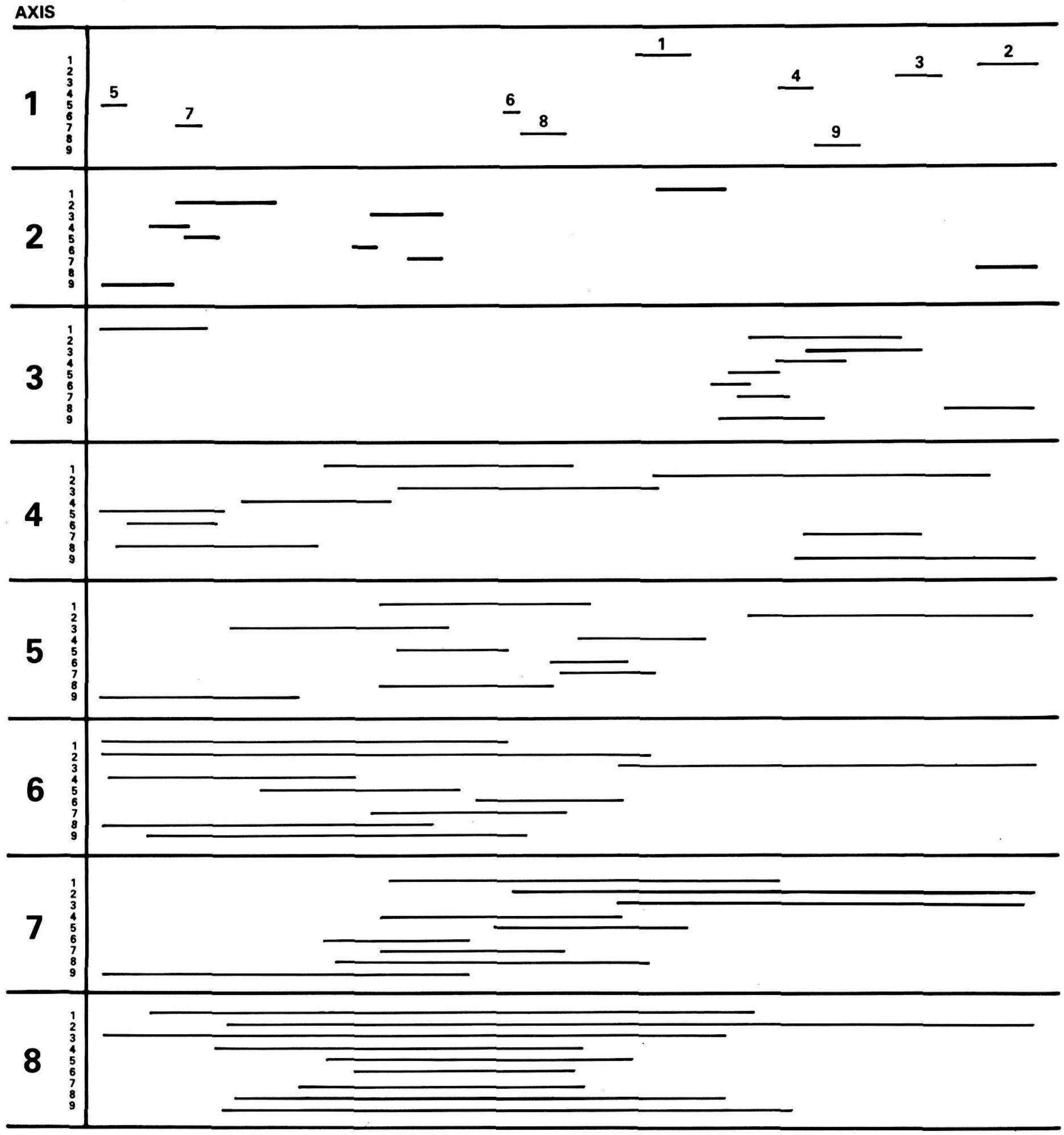

Figure 8 Canonical axes (large numbers in left column) and category separations along each axis (smaller numbers). The overlap of categories along axis 1 is minimal; whereas along 8 there is complete overlap. Categories 1, 2, 3 and 4 are defined as prehistoric; 5 is cliff; 6 is bare soil; 7 and 8 are trees; 9 is grass.

The separability of categories within each axis (fig. 8) shows that in the first axis all categories can be distinguished. The eighth axis shows the opposite; there is no separability among any of the categories. The first category of cultural sites is distinctly separable along the first 3 axes. Sites 2 and 4 are separable along the first axis, but overlap in part with the "cliff" and "grass" categories on axis 2. They are not separable along the third axis. Site number 3 is separable along the first axis but overlaps with "bare soil" and "trees" in axis 2. Like sites 2 and 4, site 3 is not separable along axis 3. Whatever the nature of the disturance at site 1, it appears to be spectrally unique from other sites and terrain categories. The separability of sites 2, 3, and 4 along the first axis is interpreted to indicate different types of past cultural activity, which through passage of time, are physically and biologically nearing their preoccupation state. Clearly, further analysis of the data and field inspection are called for.

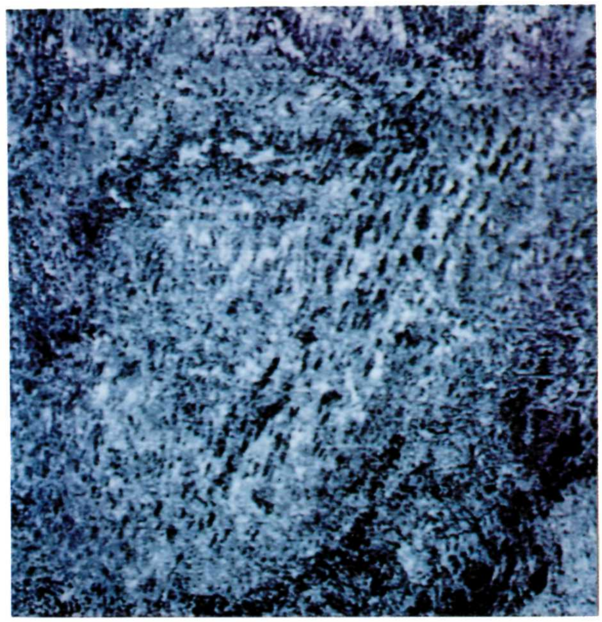

Figure 9 "Probability" image based on a maximum likelihood classifier. The darkest values have a probability of correct assignment of 99%; the largest values have a 0% confidence.

Maximum Likelihood Classification

A maximum likelihood classifier was used to group the image data into the same nine classes as were used in the canonical analysis. This classifier uses the statistical mean and covariance of the data within the training areas (fig. 7) to compute the probability (likelihood) of the multispectral data represented by a picture element belonging to a particular class. Then the element is assigned to the class in which it has the greatest probability (likelihood) of belonging. Classified and probability images are then written for display and further use.

The probability image (fig. 9) can be used to determine areas of statistically correct assignment (dark areas) or areas which are likely to have a poor statistical assignment (light areas) and so may not be adequately described in the training statistics. A qualitative interpretation of the figure suggests that a majority of pixels have high probabilities; however, only about 30–40 percent of the pixels have probabilities above 50 percent. The low probabilities may be attributed to using only 3 channels (4, 9, 11) of the original data.

Figure 10 shows thematic maps of the nine terrain categories of the classified image. There appear to be common spatial patterns between categories 2 and 3, and, to lesser extent, between 4 and 6. These represent three of the prehistoric sites and bare soil. This is an expected result considering the scarcity of vegetation and the likelihood that disturbed areas in a low rainfall environment revegetate slowly. The easiest method of comparing the distributions, however, is to combine them into a single color composite (fig. 11).

The most interesting pattern in Figure 11 is the distribution of yellow-orange spots indicated by the letters A through E. Two of these (A and B) coincide in size and location with training categories 3 and 2 in the original data set. These are reported on the Frijoles quadrangle as prehistoric. Sites C, D, and E are not listed as having been disturbed. Figure 11, therefore, is considered as an encouraging result. It leads us to an interim rejection of the null hypothesis that sites cannot be discriminated using a supervised approach. Figure 12 shows a more natural rendition of the study area with the prehistoric category 2, in white superimposed on a channel 4, 9, and 11 (blue, green and red respectively) color composite.

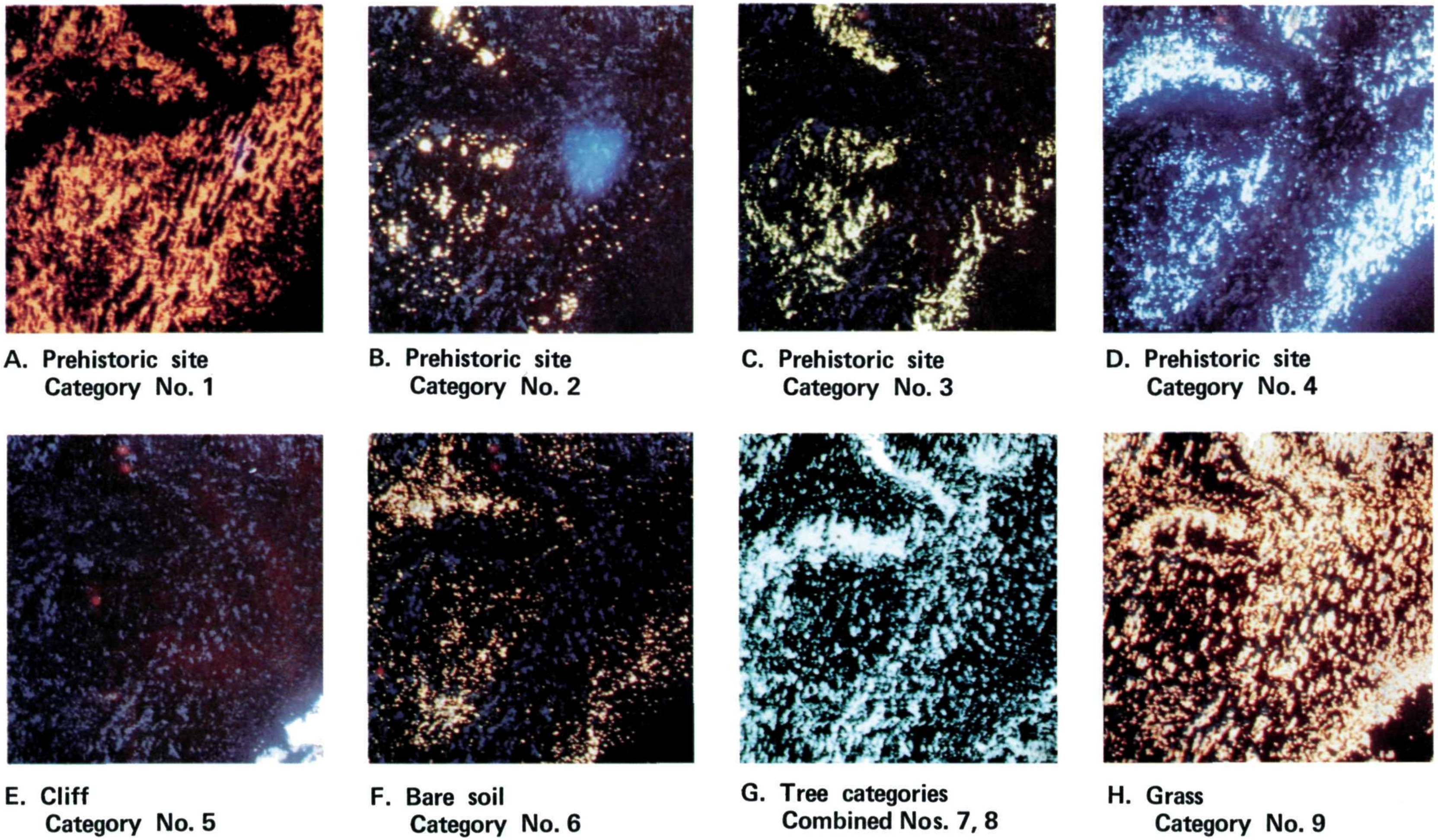

Figure 10 Color enhancements of training categories. These thermatic images show the nine terrain categories as obtained from the "supervised" maximum likelihood classifier.

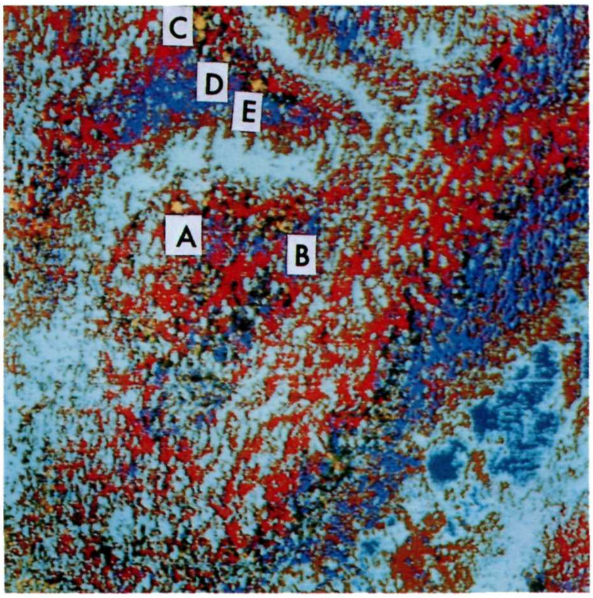

Figure 11 Nine category color combination. Note the small patches of intense yellow-orange. These coincide at A and B with known prehistoric sites. Additional possible sites are indicated at C, D and E. Yellow-oranges = prehistoric sites; dark blue = base soil and rock face; grey-green = trees; red = grass; brownish-red = undetermined.

Figure 12 Prehistoric category #2 in white superimposed on a channel 4, 9, 11 color composite in blue, green and red, respectively.

Section 3

Field Verification

The results of the maximum likelihood analysis shown in Figure 11 were field verified in July, 1978. The study area was traversed to locate as many prehistoric sites as possible. All sites were then plotted onto 1:6,000 scale, black-and-white aerial photographs. The resolution of the photographs was adequate for locating known sites. An attempt was then made to correlate those sites with the classes shown in yellow-orange on Figure 11.

The images produced by the analysis have not been geometrically corrected to match the scale or accuracy of the 1:24,000 scale topographic map. Their interpretation, therefore, depends on using relative geographic position for matching spectral response to actual locations on the ground. Further refinement of the data to register to a topographic map and to quantify the geometric root-mean-square (RMS) error needs to be undertaken to correct the image geometry.

From our field verification, it appears that the maximum likelihood classification analysis was able to identify many of the favored terrain locations for prehistoric sites. Several known sites occurred within the areas color coded as yellow-orange after classification. Those sites which are known to exist but which did not show up in the image are apparently in areas having different reflectances.

Section 4

Conclusions

The motivation behind the three approaches studied, not only in archeology but in other earth sciences as well, has been the desire to disprove the null hypotheses and extend the technique(s) to ever greater distances from the original study site. Regardless of our results, one should be cautious about the validity of signature extension. Ephemeral parameters of both scanner and terrain work together to preclude extension to any great distance. What is discriminable at one study site may not be at another because of slight differences in slope, lithology, solar azimuth, elevation, and a host of other reasons. All the conclusions must be phrased in terms of the null hypotheses. Any further conclusions have to be in terms of environmental and cultural uniformity, assuming nearly identical flying conditions and sensor performance.

In terms of the null hypotheses, "prehistoric sites cannot be visually discriminated by spectral properties alone," and "prehistoric sites, even if ground data is used to direct the enhancement, cannot be visually discriminated by spectral properties." It is concluded in this study that there appears to be no uniquely discriminable spectral signature for prehistoric areas using this data set, and an "unsupervised" enhancement approach and visual interpretation. However, a "supervised" enhancement approach or a maximum likelihood classification technique can be used with visual interpretation to discriminate prehistoric areas.

Selected References

CLARK, D.

1975 *Understanding Canonical Correlation Analysis.* In Concepts and Techniques in Modern Geography, No. 3, Institute of British Geographers, London.

DAULTRY, S.

1976 *Principal Components Analysis.* In Concepts and Techniques in Modern Geography, No. 8, Institute of British Geographers, London.

HANSON, H.C.

1962 *Dictionary of Ecology*, The Catholic University of America, Washington, D.C.

MORAIN, S.A., T.K. BUDGE, AND A. KOMAREK

1977 *An Airborne Spectral Analysis of Settlement Sites in Chaco Canyon*, Technology Application Center, UNM, prepared for remote sensing project, National Park Service, Chaco Canyon.

RUMMEL, R.J.

1970 *Applied Factor Analysis*, Evanston, Northwestern University Press.

TUAN, Y.F., C.E. EVERARD, J.G. WIDDISON, AND I. BENNETT

1973 *The Climate of New Mexico*, Revised Edition, New Mexico State Planning Office, Santa Fe.

WING, A.

1961 *Bandelier National Monument*, New Mexico National Park Service Historical Handbook Series No. 23, National Park Service, Washington, D.C.

APPENDIX A

Manufacturer	Model	Channels	Spatial Resolution	FOV	Temp. Resolution	Cost	Display
Bendix Aerospace Systems	LN-3	8–13 μm	2.5 mr 2.5 ft/1000 ft	±60°	0.1° C	Lease only	70 mm Film
	(M^2S)	10 in visible and near IR 1 at 8–14 μm	2.5 ft/1000 ft	±50°	0.5° C	$180,000	Magnetic Tape
Daedalus Enterprises, Inc.	DS 1260	10 in visible and near IR 1 at 8–14 μm	2.5 ft/1000 ft	±42°	0.2° C	Channels: 1–$200K 11–$250K	Digital on Magnetic Tape
	DS 1250	10 in visible and near IR 1 at 8–14 μm	2.5 ft/1000 ft	±39°	0.2° C	Earlier Version Special Order Only	Analog on Magnetic Tape
AGA	750	2–5.6 μm	3.4 ft/1000 ft	20° × 20°	0.2° C	$40,000	Direct Video
	680 LW	7–12 μm	2.5 ft/1000 ft	25° × 25°	0.2° C	$62,000	Direct Video
Texas Instruments, Inc.	RS–310	3–5 μm or 8–14 μm	1 ft/1000 ft	±50°	0.2° C	About $100,000	70 mm Film or Magnetic Tape (analog or digital)

Source: Aerodyne Research, Inc., Advanced Development Division, Final Report, Contract No. EX–76–C–01–2109, Report No. ARI–ADD–77–1, 12 April, 1977. "Infrared Thermography Requirements Study for Energy Conservation," pp. 4–27.

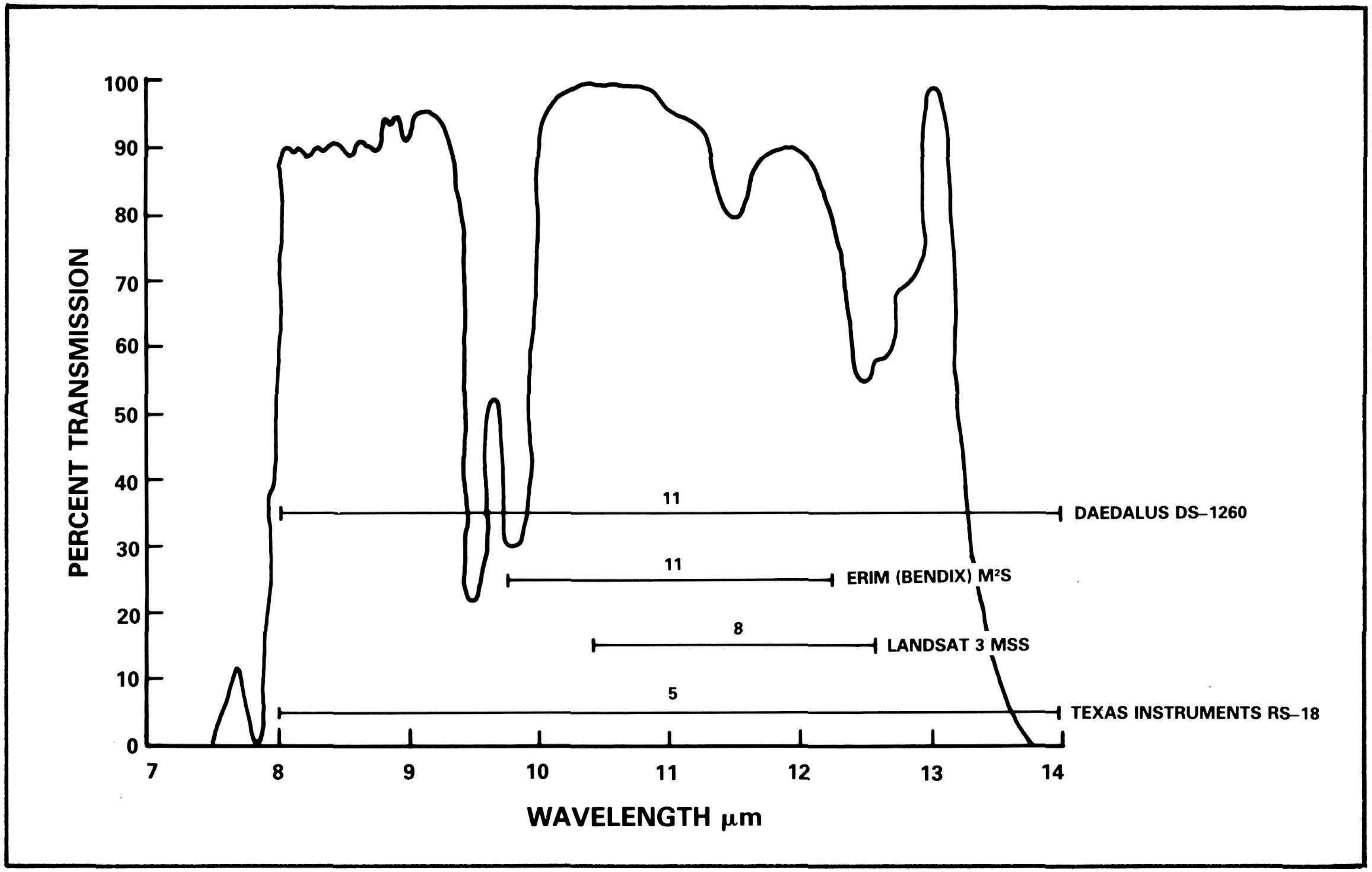
PERCENT TRANSMISSION
100
90
80
70
60
50
40
30
20
10
0
7
8
9
10
11
12
13
14
WAVELENGTH μm
11
DAEDALUS DS–1260
11
ERIM (BENDIX) M²S
8
LANDSAT 3 MSS
5
TEXAS INSTRUMENTS RS–18

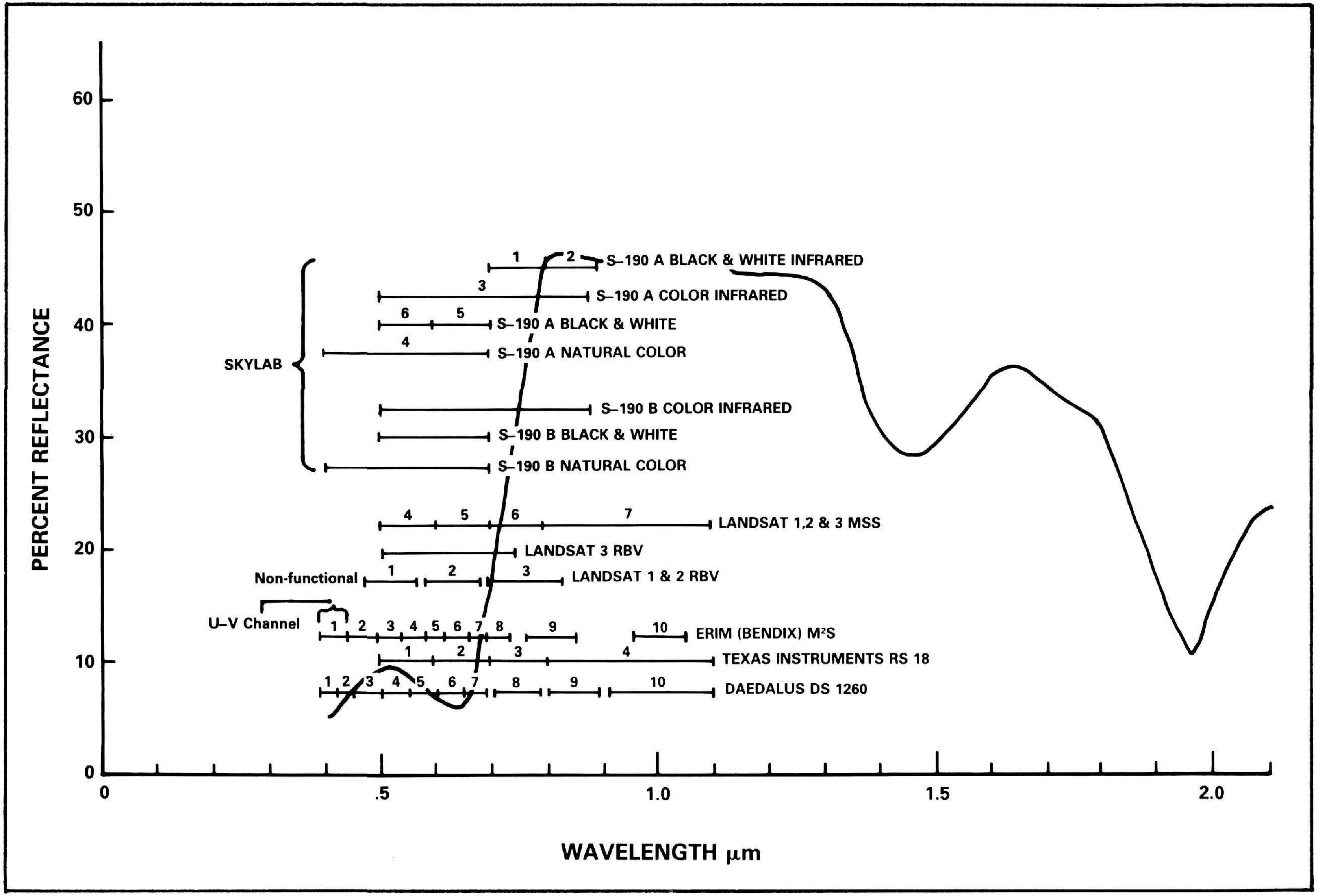
PERCENT REFLECTANCE
WAVELENGTH μm
0
10
20
30
40
50
60
.5
1.0
1.5
2.0
SKYLAB
S–190 A BLACK & WHITE INFRARED
S–190 A COLOR INFRARED
S–190 A BLACK & WHITE
S–190 A NATURAL COLOR
S–190 B COLOR INFRARED
S–190 B BLACK & WHITE
S–190 B NATURAL COLOR
LANDSAT 1,2 & 3 MSS
LANDSAT 3 RBV
Non-functional
LANDSAT 1 & 2 RBV
U–V Channel
ERIM (BENDIX) M²S
TEXAS INSTRUMENTS RS 18
DAEDALUS DS 1260

As the Nation's principal conservation agency, the Department of the Interior has responsibility for most of our nationally owned public lands and natural resources. This includes fostering the wisest use of our land and water resources, protecting our fish and wildlife, preserving the environmental and cultural values of our national parks and historical places, and providing for the enjoyment of life through outdoor recreation. The Department assesses our energy and mineral resources and works to assure that their development is in the best interests of all our people. The Department also has a major responsibility for American Indian reservation communities and for people who live in Island Territories under U.S. administration.